Check for updates

Water Resources Research

RESEARCH ARTICLE
10.1029/2023WR035360

Evapotranspiration Dynamics and Partitioning in a Grassed Vineyard: Ecophysiological and Computational Modeling Approaches

Flávio Bastos Campos[1], Torben Oliver Callesen[1], Carina Verónica Gonzalez[2,3], Giorgio Alberti[1,4], Leonardo Montagnani[1], Massimo Tagliavini[1], Jacob A. Nelson[5], and Damiano Zanotelli[1]

[1]Faculty of Science and Technology, Free University of Bolzano, Piazza Università 1, Bolzano, Italy, [2]National University of Cuyo, Mendoza, Argentina, [3]National Scientific and Technical Research Council - CONICET, Mendoza, Argentina, [4]Department of Agriculture, Food, Animal and Environmental Sciences, University of Udine, Udine, Italy, [5]Department of Biogeochemical Integration, Max Planck Institute for Biogeochemistry, Jena, Germany

Abstract Plenty of information on evapotranspiration (ET) dynamics and partitioning into nonbiological (evaporation, E) and biological (transpiration, T) components is available in literature. However, in agro-ecosystems where more than one vegetation group is found, like intercropping or grassed orchards and vineyards, it is of great use to understand the contribution to T due to the single plant type or group of plants. We deployed empirical and modeling methods to study the ecosystem evapotranspiration (ET_{EC}) components in a grassed vineyard in Caldaro (Italy) aiming to assess (a) which process, E or T, had greater influence on ET_{EC} dynamics; (b) which component among grapevines and understorey portion dominated the ET_{EC}; and (c) how rainfall influences ET_{EC} components. A top-down approach combined the eddy covariance method to estimate ET_{EC}, and the Transpiration Estimation Algorithm method to partition it. A bottom-up approach integrated the understorey evapotranspiration (ETu) with modeled vines transpiration ($Tv_{(mod)}$). Measured and modeled fluxes showed high daily variability, consistently with meteorological conditions (vapor pressure deficit, Rn and Tair). The mean daily ET_{EC} integrals were 3.45 and 3.40 mm d^{-1} (2021 and 2022), being T_{EC} (estimated transpiration fraction of ET_{EC}) the higher contributor (T_{EC}/ET_{EC} of 0.77 and 0.79, same years). From the bottom-up approach, ETu assessed during ground flux chamber campaigns (0.74–1.65 mm d^{-1}) was lower than $Tv_{(mod)}$. A high agreement ($R^2 = 0.85$) was found between the eddy covariance ET hourly values and ET by summing $Tv_{(mod)}$ and ETu. We concluded that the T process represented major fluxes in the agroecosystem during the warm season. Furthermore, the bottom-up approach indicated the vines as primary contributors to ecosystem T, particularly noticeable after rainfall, as the understorey T fraction (Tu) increased when the system became drier. This study helps disentangling grapevine contribution to evapotranspiration from adjacent herbaceous vegetation in a vineyard, and emphasizes the dominance of biologically mediated transpiration influenced by meteorological conditions. This novel combination of approaches not only enhances understanding of Mediterranean viticulture but also illuminates broader applications in sparsely vegetated environments, such as agroforestry systems and orchards, advancing ecological management practices.

Key Points:

- Top-down partitioning of eddy derived ET_{EC} via Transpiration Estimation Algorithm algorithm showed a dominance of T with respect to E over the vineyard water fluxes
- The bottom-up approach demonstrated a generally higher contribution of vines T with respect to understorey fluxes on total ET_{EC}
- E reached up to 31% of total ET_{EC} on the first day after a precipitation event, decreasing later on to only 14% on the third day

Supporting Information:

Supporting Information may be found in the online version of this article.

Correspondence to:

Damiano Zanotelli,
damiano.zanotelli@unibz.it

Citation:

Bastos Campos, F., Callesen, T. O., Gonzalez, C. V., Alberti, G., Montagnani, L., Tagliavini, M., et al. (2025). Evapotranspiration dynamics and partitioning in a grassed vineyard: Ecophysiological and computational modeling approaches. *Water Resources Research*, *61*, e2023WR035360. https://doi.org/10.1029/2023WR035360

Received 15 MAY 2023
Accepted 14 JAN 2025

Author Contributions:

Conceptualization: Flávio Bastos Campos, Carina Verónica Gonzalez, Leonardo Montagnani, Massimo Tagliavini, Jacob A. Nelson, Damiano Zanotelli
Data curation: Flávio Bastos Campos, Carina Verónica Gonzalez, Giorgio Alberti, Leonardo Montagnani, Damiano Zanotelli
Formal analysis: Flávio Bastos Campos, Torben Oliver Callesen, Giorgio Alberti,

© 2025. The Author(s). *Water Resources Research* published by Wiley Periodicals LLC on behalf of American Geophysical Union.
This is an open access article under the terms of the Creative Commons Attribution License, which permits use, distribution and reproduction in any medium, provided the original work is properly cited.

1. Introduction

Irrigation is used in approximately 30% of all Mediterranean cultivation systems (FAO, 2016), wherein viticulture plays a significant role in the regional water cycle. The need for irrigation in these areas has grown due to climate change, which intensifies water scarcity and necessitates irrigation to maintain grape yield and quality (Teuling et al., 2009; Wenter et al., 2018). While irrigation increases economic costs, it also offers environmental benefits such as enhancing moisture recycling and potentially decreasing regional air temperatures (De Hertog et al., 2023; Thiery et al., 2020), in contrast with non-irrigated crops which tend to cause further drying in water circulation, amplifying heat waves (Miralles et al., 2018). Understanding the water needs and dynamics of Mediterranean crops, particularly in the case of vineyards with co-occurring vegetation, is essential to sustainable implementation of necessary measures in these water-scarce regions.

Among the most studied components of the water cycle in agricultural ecosystems are the biological (transpiration, T) and nonbiological (evaporation from soil and intercepted water, E) fluxes of water to the atmosphere. The sum of both processes, often denominated as evapotranspiration (ET = T + E), is a relevant flux of the water

19447973, 2025, 3, Downloaded from https://agupubs.onlinelibrary.wiley.com/doi/10.1029/2023WR035360 by CochraneItalia, Wiley Online Library on [28/03/2025]. See the Terms and Conditions (https://onlinelibrary.wiley.com/terms-and-conditions) on Wiley Online Library for rules of use; OA articles are governed by the applicable Creative Commons License

Leonardo Montagnani, Jacob A. Nelson, Damiano Zanotelli
Funding acquisition: Massimo Tagliavini, Damiano Zanotelli
Investigation: Flávio Bastos Campos, Torben Oliver Callesen, Carina Verónica Gonzalez, Leonardo Montagnani, Damiano Zanotelli
Methodology: Flávio Bastos Campos, Carina Verónica Gonzalez, Leonardo Montagnani, Massimo Tagliavini, Damiano Zanotelli
Project administration: Massimo Tagliavini, Damiano Zanotelli
Resources: Giorgio Alberti, Massimo Tagliavini
Software: Jacob A. Nelson
Supervision: Carina Verónica Gonzalez, Leonardo Montagnani, Massimo Tagliavini, Jacob A. Nelson, Damiano Zanotelli
Validation: Flávio Bastos Campos, Giorgio Alberti, Massimo Tagliavini, Jacob A. Nelson, Damiano Zanotelli
Visualization: Carina Verónica Gonzalez, Leonardo Montagnani, Massimo Tagliavini, Jacob A. Nelson, Damiano Zanotelli
Writing – original draft: Flávio Bastos Campos
Writing – review & editing: Flávio Bastos Campos, Torben Oliver Callesen, Carina Verónica Gonzalez, Giorgio Alberti, Leonardo Montagnani, Massimo Tagliavini, Jacob A. Nelson, Damiano Zanotelli

balance in agroecosystems (Villalobos & Fereres, 2016). While E depends on surface water availability and environmental factors such as solar radiation, relative humidity, air temperature and wind speed, T corresponds to the transfer of water vapor from inside the leaves to the atmosphere and is additionally controlled by stomatal resistance (Allen et al., 1998). Due to the complex mechanisms controlling both processes, their relative contribution to ET may vary sensibly based on the agroecosystem type, the crop management practices, and the short-term change in weather conditions, including wetting events, which are still poorly understood and often not integrated into current models.

A prominent method to assess ecosystem-scale water vapour fluxes is eddy covariance, which makes it possible to quantify CO_2 and water vapour fluxes by the covariance between gas concentrations and the vertical wind speed (Baldocchi et al., 1988). The estimated water vapour fluxes refer to the ecosystem evapotranspiration (ET_{EC}), consisting of high frequency measurements of eddies originating at various points within the flux footprint, then averaged for every half hour to produce a continuous time series of ecosystem-scale values (Burba, 2013).

However, eddy covariance does not provide direct measurements of E and T components separately. Indeed, understanding the separate contribution of the different sources is crucial for agricultural sciences and food production, as well as for the comprehension of the link between the hydrological and carbon cycles, which can enhance models by constraining them and improve strategies to address both hydrological and carbon cycling processes, crucial in the context of climate change and agricultural demands (Shuttleworth & Wallace, 1985). Although ET has been simply referred as the sum of T and E (Stoy et al., 2019; Wei et al., 2018), partitioning ET at farm- or ecosystem-level is a complex task since water vapour originates from different sources, for example, crop, below-crop soil and below-canopy vegetation (also referred as understorey), each of which are exposed to different microclimates (Klosterhalfen et al., 2019; Paul-Limoges et al., 2020). Understanding the specific contribution of each of these sources to crop ET requires field data from eddy covariance sites and repositories for ancillary data, valid assumptions to enable hypothesis testing, and an applicable methodology to ensure effective integration of data and model development (Scanlon & Kustas, 2010; Stoy et al., 2019). There is currently no single consolidated procedure to partition ET (Paul-Limoges et al., 2020, 2022), but multiple methods have been developed in recent years. These methods utilize site eddy covariance data and aim at estimating T from ET, generally with good agreement regarding temporal patterns but differing in the magnitude of T (Scott et al., 2021). Variability in T/ET ratios are found to be dependent of the plant functional type (Nelson et al., 2020), ranging in the intervals of 0.56–0.78 (natural plants), 0.36–0.78 (deciduous broadleaf forests), 0.38–0.67 (grasslands), 0.25–0.61 (evergreen needleleaf forests), and 0.33–0.45 (woody savannas) (Yu, Zhou, et al., 2022). For this reason, including additional measurements can potentially reduce uncertainties.

Among the available ET partitioning models, being mechanistic (e.g., physiological or physical based) or machine learning based, the most commonly adopted ones have good performance within the assumptions and context under which they were developed. However, some models partitioning ET into T + E at ecosystem scale disregard the contribution of the single sources of water fluxes (Kool et al., 2016; Wei et al., 2018). In fact, permanent crops quite often include two or more types of vegetation (i.e., main crop and cover crop) and differentiating the contribution of water vapour from each component of the ecosystem is a key element to improve management strategies and assess the vegetation water requirement needed to meet the expected ecosystem service or productivity (Poblete-Echeverría & Ortega-Farias, 2013; Zhao, Hammerle, et al., 2018). In vertically heterogeneous environments, there are multilayer canopy models able to incorporate essential interactions of the above and belowground ecohydrological dynamics and biochemical functioning among multiple species, considering multiple layers and their interplay with environmental factors. These integrate physiological processes and environmental variables across different canopy layers (e.g., MLCan, https://github.com/Hydro-Complexity/MLCan2.0), representing ecosystem dynamics, including water, energy, carbon, and nutrient cycles (e.g., ECOSYS, https://github.com/jinyun1tang/ECOSYS) and simulating the gross canopy photosynthesis within many layers considering light distribution (e.g., MAESPA, Duursma & Medlyn, 2012; Linderson et al., 2012).

To face the challenge posed by the coexistence of multiple layers of vegetation in the same agroecosystem, several empirical methods have been recently employed. Principle crop transpiration at single leaf to plant level can be measured with different techniques including measurement of stomatal conductance by porometry or gas exchange, isotopic tracer methods and heat tracer-based sap flow techniques (SF) (Zhang et al., 2011; Mancha et al., 2017). The SF method has been evaluated and demonstrated to be effective in several species including

19447973, 2025, 3, Downloaded from https://agupubs.onlinelibrary.wiley.com/doi/10.1029/2023WR035360 by CochraneItalia, Wiley Online Library on [28/03/2025]. See the Terms and Conditions (https://onlinelibrary.wiley.com/terms-and-conditions) on Wiley Online Library for rules of use; OA articles are governed by the applicable Creative Commons License

grapevines (Ferreira et al., 2012; Kool et al., 2016; Poblete-Echeverría & Ortega-Farias, 2013; Zhang et al., 2011), especially using the heat balance method described by Sakuratani (1981) (Gao et al., 2019; Zhao, Kang, et al., 2018), and can be upscaled from plant-to ecosystem-scale by multiplying SF per plant to the average ground surface per plant. This is a common proxy to estimate the T component of an ecosystem, with the advantage of providing a continuous time series.

The understorey fluxes (ET_u), also referred to as below-canopy flux, play a significant role in the ecosystem dynamics (Paul-Limoges et al., 2020; Qubaja et al., 2020), and complement the information obtained with sap flow sensors making a stronger approach towards closing the water balance in the ecosystem. These may be estimated by lysimeters (Sánchez et al., 2019), water balance calculations (Helbig et al., 2013) or automated transparent flux chambers (McLeod et al., 2004; Qubaja et al., 2020; Simpson et al., 2019). The last comprises robust equipment, able to endure environmental conditions and can integrate into existing field experiment set-ups, especially in environments with bare soil or short vegetation (Varolo et al., 2016). Mounted onto pre-installed collars, the flux chambers enclose a defined soil area, establishing a controlled environment within which to assess the exchange of gases (e.g., CO_2 and water vapour), between the ground-level portion and the atmosphere (Cohen et al., 2015; Qubaja et al., 2020). Once the chamber is closed, air is directed to an infrared gas analyzer where gases concentrations are precisely measured and their variation used to compute fluxes (Raz-Yaseef et al., 2010; Simpson et al., 2019). The data obtained refers to a small scale (collar-scale, ca. 300 cm^2) that can be upscaled to provide good flux estimations if care is taken towards the method's limitations (see Livingston & Hutchinson, 1995), such as when applying the regression to obtain the fluxes (Simpson et al., 2019), selecting the proper time interval (McLeod et al., 2004), and filtering for conditions that favour dew formation (Paulus et al., 2022).

In the present study we approached the partitioning of the ecosystem ET from a grassed vineyard into its main components by means of an innovative protocol combining two distinct approaches: a top-down procedure consisting of measuring the bulk ecosystem ET_{EC} and partitioning it to obtain the ecosystem-level transpiration (T_{EC}), and a bottom-up approach where ET is obtained by summing vine transpiration and understorey water flux. Both approaches were deployed in a complex tree-grass vineyard ecosystem to assess water fluxes, seeking to shed light on both E and T processes along two growing seasons and, in a shorter time scale, on modification of their relative contribution to ET when the system gets drier after a rainfall event. Although this analysis used a grassed vineyard as a model site, it offers a perspective on the ecological dynamics of water vapour fluxes applicable to several agro-ecosystems organized in at least two main layers where the lower consists of structured soil covered by herbaceous vegetation and the upper of woody crop species. Such organization is gaining attention and becoming common structure in Mediterranean orchards (e.g., apples, citrus, walnuts, olives) geared towards improving the sustainability and resilience of the agroecosystems through the promotion of biodiversity and other ecosystem services, as well as the increase of soil stability and quality (Abdalla et al., 2019; Tamburini et al., 2020; Van Eerd et al., 2023; Vuckicevic et al., 2016).

The goals of this study were to partition ET into T and E components and obtain further insights into the contribution of different components of the considered agroecosystem. More specifically, by combining ET components assessed by the two approaches, we aimed to answer the following questions: (a) which of the two processes, E and T, has a greater influence on vineyard ET dynamics and how do their contributions vary over the course of the primary growing season? (b) Which component among the grapevines and the understorey portion dominates ET? (c) What is the influence of rainfall events on the component water fluxes?

2. Materials and Methods

2.1. Water Flux Partitioning Approaches

Two approaches were employed to estimate water fluxes: 1st—the top-down approach using the eddy covariance to assess the ecosystem evapotranspiration as whole without distinction of each source or component (ET_{EC}), and the Transpiration Estimation Algorithm (TEA) algorithm (Nelson et al., 2018) to partition ET_{EC} into T_{EC} and E_{EC} ecosystem components; 2nd—the ecophysiological approach (EPA). This involves estimating water fluxes from vine transpiration (Tv) and understorey evapotranspiration (ETu), which are then combined assuming negligible canopy evaporation (Ev), to calculate ecosystem-scale evapotranspiration (referred to hereafter as ET_{EPA}). Figure 1 illustrates a perspective of both methods. Refer to Figure S1 in Supporting Information S1 for the field organization scheme.

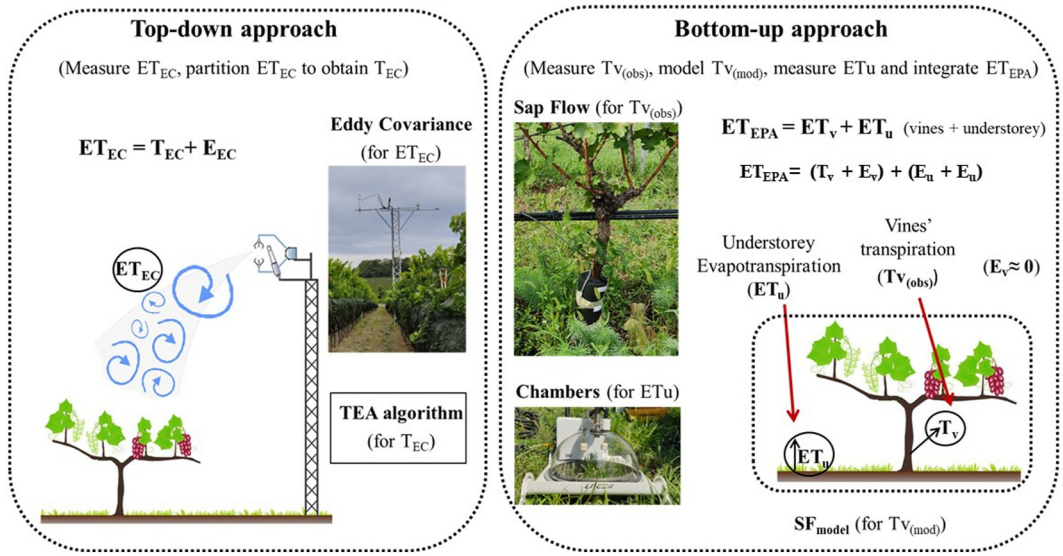

Figure 1. The two deployed approaches to obtain water fluxes from components of the ecosystem. 1st: as a top-down approach, the eddy covariance to measure the ecosystem evapotranspiration (ET_{EC}), and the Transpiration Estimation Algorithm algorithm to partition it and obtain T_{EC}; 2nd: the ecophysiological approach—EPA—to measure or estimate the water fluxes of the vines transpiration (Tv) and the understorey evapotranspiration (ETu), which were added to obtain the ecosystem evapotranspiration by EPA (ET_{EPA}).

Following the top-down approach, ET_{EC} was partitioned according to Equation 1:

$$ET_{EC} = E_{EC} + T_{EC} \quad (1)$$

In the EPA (bottom-up approach), components from different sources (ET_{EPA}) were summed, as in the hydrological budget (Qubaja et al., 2020):

$$ET_{EPA} = T_v + E_v + T_u + E_u \quad (2)$$

where Tv is the vines' transpiration (being the observed $Tv_{(obs)}$ or the modeled $Tv_{(mod)}$), Tu is the understorey vegetation transpiration, E_u is the understorey vegetation and soil evaporation and the Ev is the rain evaporated after canopy interception, which was assumed to be negligible. This assumption holds to the Bottom-up approach in order to make it possible to apply Equation 2 to the vineyard experimental context. A detailed description of all the methods and models indicated in Figure 1 is reported in the following sections, while a deeper discussion of the main uncertainties related to each of them are included in the supplemental material (Text S1 in Supporting Information S1. Limitations and uncertainties).

2.2. Experimental Site

This study was conducted in a hillside vineyard in Kaltern-Caldaro, South Tyrol (46° 44′ N, 11° 13′ E, 325 m a.s.l.) in northern Italy, from May 2021 to September 2022. The experimental vineyard was 0.85 ha in size, with homogeneous terrain and a 5% slope. The surrounding area was also predominantly used for grapevine cultivation.

The region has a temperate climate (Cfb according to the Köppen-Geiger classification). The vineyard was established in 2008, on sandy loam soil (57.4% sand, 28.4% silt and 14.2% clay; 2.4% of organic matter, and 0.29 of fraction of stones, in volume).

Two *Vitis vinifera* L. cultivars were present: Chardonnay (with inter-rows 2.0 m wide and inter-vine spacing of 0.75 m; 6,667 vines ha^{-1}) and Sauvignon blanc (inter-rows 2.0 m wide and inter-vine spacing of 0.80 m; 5,882 vines ha^{-1}); both grafted on SO4 rootstock, trellised to a vertical shoot positioning system and pruned as single Guyot. The vineyard had a drip irrigation system with 2.2 L hr^{-1} drippers placed every 0.80 m along the lines, in

19447973, 2025, 3, Downloaded from https://agupubs.onlinelibrary.wiley.com/doi/10.1029/2023WR035360 by CochraneItalia, Wiley Online Library on [28/03/2025]. See the Terms and Conditions (https://onlinelibrary.wiley.com/terms-and-conditions) on Wiley Online Library for rules of use; OA articles are governed by the applicable Creative Commons License

19447973, 2025, 3, Downloaded from https://agupubs.onlinelibrary.wiley.com/doi/10.1029/2023WR035360 by CochraneItalia, Wiley Online Library on [28/03/2025]. See the Terms and Conditions (https://onlinelibrary.wiley.com/terms-and-conditions) on Wiley Online Library for rules of use; OA articles are governed by the applicable Creative Commons License

between the vines on the same row. The irrigation management was decided by a consortium and applied for vineyards in the region. The site has been managed since 2009 according to EU organic farming guidelines.

A system of alternate cover cropping was used, whereby every second inter-row was tilled to a depth of 5 cm and planted in Autumn with a mix of cover crop seeds (composed by Dańkowskie Rubin rye (*Secale cereale*, 40%), hairy vetch (*Vicia villosa*, 40%), incarnate clover (*Trifolium incarnatum*, 10%), and sainfoin (*Onobrychis viciifolia*, 10%)). These crops were then allowed to grow and are mown once at the end of the following grapevine growing season (from May to end of September). Adjacent inter-rows were left to be covered by spontaneous grasses (such as *Lolium multiflorum* Lam., *Trifolium repens* L. and *Cynodon dactylon* (L.) Pers.), which were periodically mowed during the year. The ground strip under the vines of 0.40 m wide was also covered by the above-mentioned grasses, with the addition of spontaneous species, for example, *Artemesia vulgaris* L. *Salvia pratensis* L., *Taraxacum officinale* W. and *Urtica dioica* L. Of note, the grapevine underline was mechanically cleared with each mowing event.

An annual fertilization was performed with an average of 0.125 kg per plant of an organic fertilizer containing 80% organic matter, N, P and K. Budburst occurred in early April, veraison in early August and harvest in mid-September.

2.3. Instrumentation

2.3.1. Eddy Covariance for Ecosystem Evapotranspiration (ET_{EC})

The experimental site was selected because of the favorable conditions for eddy covariance measurements, and this method was used to assess the ecosystem evapotranspiration (ET_{EC}). The terrain was homogeneous in terms of the topography, with a slope of about 5%. The experimental area was surrounded by other vineyards, allowing an adequate fetch for all wind directions.

A tower was installed to support the eddy covariance equipment and a series of meteorological instruments. A 3-dimensional ultrasonic anemometer (Gill R3-50, Gill Instruments, Lymington, UK) and a close-path IR gas analyzer (LI-COR LI-7200, LI-COR Biosciences Lincoln, NE, USA) were set at 6 m above the ground. Air samples were taken through an insulated steel tube of 4 mm in internal diameter and 0.75 m in length at 0.2 m from the anemometer. The airflow rate was within the range of 10–12 L min^{-1}, as provided by the flow module (7200-101, LI-COR Biosciences, Lincoln, NE, USA).

Measurements were recorded from May 2021 to September 2022, covering most of the grapevine growing seasons (May to end of September) in 2021 and 2022. Raw values of CO_2 and H_2O concentration (in units of µmol mol^{-1} and mmol mol^{-1}, respectively) and 3D wind speed components were measured at 20 Hz and logged by a PC every 30 min using the EddyMeas software package (Kolle & Rebmann, 2007). Data containing net ecosystem exchange, sensible heat (H), latent heat (LE) and friction velocity (u_*) were processed at half-hourly scale using the Eddysoft (within EddyMeas). Data were screened out according to the Foken and Wichura (1996) quality test for turbulence and stationarity. The footprint was obtained using the Flux Footprint Prediction online tool (detailed in Kljun et al., 2015). The area included 90% of the flux source, with length and width of ±200 m and ±100 m, respectively, presenting an oval shape centered in the tower, oriented south-east (image available in Callesen et al., 2023).

To address the energy imbalance, the energy balance closure (EBC) was forced on monthly intervals, following the "method #4" in Wohlfahrt et al. (2009). In this approach the residual energy is attributed with proportional weight to both LE and H. Therefore, the computation generates the monthly energy balance ratio (EBR) values, which were applied to correct the H and LE fluxes, allowing the energy budget to close and ET_{EC} to be corrected for this site, the turbulent fluxes were only slightly underestimated with the EBR varying among the considered months from 0.767 to 0.988 and from 0.839 to 0.996 in 2021 and 2022, respectively (Table S1 in Supporting Information S1).

2.3.2. Sap Flow for Vines Transpiration ($Tv_{(obs)}$)

Vines transpiration ($Tv_{(obs)}$) was estimated based on field-obtained sap flow measurements. The function of the sap flow probes is based on the trunk heat balance method, as heat is applied to the whole trunk circumference which is encircled by a heating tape and the sap flow is obtained by measuring the difference in the fluxes of heat

19447973, 2025, 3, Downloaded from https://agupubs.onlinelibrary.wiley.com/doi/10.1029/2023WR035360 by CochraneItalia, Wiley Online Library on [28/03/2025]. See the Terms and Conditions (https://onlinelibrary.wiley.com/terms-and-conditions) on Wiley Online Library for rules of use; OA articles are governed by the applicable Creative Commons License

into and out of the trunk's heated section (Peressotti & Ham, 1996; Sakuratani, 1981). The lab-made system has operated since 2000, and was calibrated and validated in previous studies (Tricker et al., 2009).

These measurements were performed using sap flow probes installed on 3 grapevines, one sensor per plant, at approximately 10 cm above the grafting point (mean trunk diameter section of 29.6 ± 1.2 mm) within the eddy covariance tower's footprint. Data collection was from June to the end of August 2022, when the probes were in operation logging data in g of water per plant ($SF_{g/p}$) every half-hour via a connected CR1000 datalogger (Campbell Scientific Incorporated (CSI), Logan, Ut, US). The fluxes were upscaled to mm hh^{-1} as in Zhao et al. (2015):

$$Tv_{(mm/hh)} \sim SF_{mm/hh} = \frac{SF_{g/p}}{10^3 \, \rho_{H_2O} \, A_p} \quad (3)$$

where $\rho_{H_2O} = 0.997$ g cm^{-3} is the water density at 25°C and $A_p = 1.85$ m^2 $plant^{-1}$ is the average ground surface per grapevine. Assuming the sap flow to be a proxy for the vine transpiration, we integrated the obtained fluxes into hourly and daily scales. Vine transpiration time series obtained for the three plants was averaged for further data analysis.

2.3.3. Transparent Ground-Level Chambers for Understorey Evapotranspiration (ETu)

The grapevine's understorey is a fraction of the ecosystem that contributes to the whole ET_{EC} in an important way, particularly in this site where the ground level vegetation is managed by the farmer. The contribution of this fraction to the ET_{EC} comprises the understorey vegetation's transpiration (Tu), and the evaporation of the free water from its surface and the soil (Eu):

$$ET_u = T_u + E_u \quad (4)$$

Measuring these components individually, in situ, without interfering radically to the soil or vegetation structure and microclimate is experimentally challenging. Therefore, the field assessment of ETu was done using transparent ground-level chambers, and was organized in a campaigns format to take into account the temporal and spatial variability of ETu, as well as the traffic of machines related to farmers' activities in the vineyard, for example, spraying, mowing grass, tillage and green manure incorporation.

A total of 5 campaigns took place from July to September 2021, each organized to start in the morning and last around 72 hr. Individual campaigns relied on three transparent chambers (Long-Term Chambers; LI-8100-104C; LI-COR Biosciences, Lincoln, NE, USA), mounted on steel collars (diameter: 20 cm, height: 10 cm) inserted to a depth of 7 cm in the soil. The chambers were connected to a multiplexing system (Multiplexer; LI-8150; LI-COR) to allow for the simultaneous control of several chambers via 10-m-long tubing, which was in turn connected to a gas analyzer (LI-8100A; LI-COR). During campaigns, each chamber was moved to a new position with an unoccupied, pre-installed collar every 24 hr (three times per campaign) for better spatial representation. This way, the campaigns took place to coincide with active vegetation growth and irrigation in the vineyard, consisting of measurements over multiple campaigns that allows for capturing environmental variability and vegetation growth dynamics.

In order to have the chambers closing and encompassing all the vegetation inside the dome's area, the vegetation inside each collar's perimeter was cut off at 10 cm above the ground level, kept in individually labeled plastic bags and taken to the laboratory to assess the green leaf area ($GLA_{>10cm}$). After 24 hr, when finished the measurements at a spot the remaining ground-level vegetation was collected (the vegetation portion of <10 cm height), following the similar protocol to obtain the $GLA_{<10cm}$ (further details in Text S5.4 in Supporting Information S1).

This experimental setup was programmed to take measurements at each assessment point every 15 min, that is, at every time step, each chamber in a pre-defined sequence would close, sample the gas and send it to the gas analyzer through the multiplexer. At each sampling event the system was set to perform a pre-purge of 15 s, a post-purge of 20 s and sampling duration was 90 s, with frequency of 1 observation of water vapor concentration (mmol mol^{-1}) each second within that period. The raw data were curated using the application SoilFluxPro v4.2.1 (LI-COR Team, 2021), which allows to calculate the water vapor flux as the rate of change of the water vapor

concentration during the measurement time (mmol m^{-2} s^{-1}). The linear regression was applied to obtain the fluxes (Raz-Yaseef et al., 2010; Simpson et al., 2019), based on concentration values of the range 20–40s of the original observations (refer to Text S5.2 in Supporting Information S1 for detailed information on the decision about the used time-window of the concentration series).

Nighttime data (from 20:00 to 6:00) were removed from the analysis as well as all those data points obtained with an R^2 of the linear correlation <0.80 (Järveoja et al., 2020). This filtering allowed keeping 86% of data obtained in daytime condition (Rg > 2.5 Wm^{-2}). The estimated fluxes were then submitted to a series of corrections, first due to the water vapor adsorption in the tubing, second due to cutting off the vegetation to accommodate the chambers on collars, and last due to missing values resulting from data quality screening.

The corrections due to the tubing effect were performed using a multiplicative coefficient (1.76) obtained in an indoor calibration trial, during which the ground flux chambers were positioned on hung planted pots and the ETu measured by the chambers were contrasted against weighing lysimeters, resulting in the multiplicative coefficient to correct chamber-ETu flux values (Text S5.3 in Supporting Information S1). Regarding cutting off the vegetation to accommodate the chambers on collars, it was assumed that the ETu fluxes were linearly and directly related to the GLA, in the range of total GLA <2 m^2 m^{-2} (Alam et al., 2021; Wei et al., 2018). Then we upscaled the measured ETu from 10 cm-height vegetation to actual vineyard-floor vegetation by the multiplying ETu to $(GLA_{>10cm} + GLA_{<10cm})/GLA_{<10cm}$ for each collar (Text S5.4 in Supporting Information S1). It was assumed that most of the fluxes were captured by the measurements performed by the 10 cm-height vegetation, given that many leaves were in this layer. Moreover, the GLA index is more representative compared to others (such as dry biomass) for water vapor fluxes.

At last, the corrected fluxes were synchronized with meteorological and eddy covariance data, the missing values were filled in using the *missForest* function, from the *missForest* package (Stekhoven & Buehlmann, 2012) for open-source R software (R Core Team, 2021). This package uses random forest (Breiman, 2001) to perform nonparametric missing value imputation, trained on ETu, latent heat (LE), sensible heat (H), global radiation (Rg), vapor pressure deficit (VPD), air temperature (T_{air}), wind speed (ws), air relative humidity (rH), precipitation (Precip) and volumetric soil water content (usoil10). The corrected fluxes were averaged and upscaled to hourly time scale for the following analysis.

2.4. Models

2.4.1. Modeling the Ecosystem Transpiration (T_{EC})

In the condition when no empirical instrumentation is able to evaluate independently the transpiration component of the understorey layer, and sum it to the vines' transpiration to obtain the ecosystem transpiration, partitioning Eddy Covariance ET using a model is of great value. Within this context, the TEA method from Nelson et al. (2018) was used to partition eddy covariance ET into T and E. The algorithm first filters the data keeping periods during the growing season with GPP >0.5 gC m^{-2} d^{-1}, when the surface (soil and vegetation) is likely to be dry and E/ET is assumed to be negligible. This filter is done based on precipitation input and ET in a shallow bucket model (details in Nelson et al., 2018).

Then, a non-parametric model based on random forest (Breiman, 2001) is trained within the filtered periods, on the ecosystem WUE (WUE_{eco} = GPP/ET) using as predictors the eddy covariance fluxes (i.e., water, carbon, and energy fluxes) and meteorological data (e.g., Rg, Tair, rH and ws). The trained model predicts WUE_T (WUE_T = GPP/T) at every time step (Meinshausen, 2006). These WUE_T values are assumed to represent a single true WUE_{eco} contaminated by residual evaporation. The appropriate percentile of WUE_T values, usually the 75th, is used to adjust the magnitude of predicted WUE_T, accounting for both residual evaporation and WUE_T variability. Then, T_{EC} is obtained as T_{EC} = GPP/WUE_T. For further details, refer to Nelson et al. (2018).

The TEA method does not require carbon-water optimality assumptions, so the relation between WUE and the variables comes directly from the available data, which results in predictions that are dynamic in time (Nelson et al., 2020). In this study, the TEA model was used at a half-hourly time scale, then the resulting T_{EC} time series was integrated into hourly and daily scales.

19447973, 2025, 3, Downloaded from https://agupubs.onlinelibrary.wiley.com/doi/10.1029/2023WR035360 by CochraneItalia, Wiley Online Library on [28/03/2025]. See the Terms and Conditions (https://onlinelibrary.wiley.com/terms-and-conditions) on Wiley Online Library for rules of use; OA articles are governed by the applicable Creative Commons License

19447973, 2025, 3, Downloaded from https://agupubs.onlinelibrary.wiley.com/doi/10.1029/2023WR035360 by CochraneItalia, Wiley Online Library on [28/03/2025]. See the Terms and Conditions (https://onlinelibrary.wiley.com/terms-and-conditions) on Wiley Online Library for rules of use; OA articles are governed by the applicable Creative Commons License

Summarized key steps of the TEA:

1. Filtering: select eddy covariance data during growing seasons with GPP >0.5 gC m^{-2} d^{-1}.
2. Training a model: train a random forest model on ecosystem water use efficiency (WUE_{eco} = GPP/ET) using eddy covariance and meteorological data.
3. Calculate WUE_T (GPP/T) at each time step using the trained model.
4. Adjust WUE_T values to the 75th percentile to account for residual evaporation and variability.
5. Apply TEA model: estimate T_{EC} = GPP/WUE_T, at half-hourly scale and integrate into hourly and daily scales.

2.4.2. Modeling Vines Transpiration With Random Forest ($Tv_{(mod)}$)

Targeting to analyze which component among the grapevines and the understorey portion that dominates ecosystem ET, a data set of vines' transpiration and understorey ET was needed for the same period. To match the ETu data obtained for 2021 (refer to Section 2.3.3), vines' transpiration for the same period was simulated using a trained machine learning model (SF_{model}) based on the random forest algorithm (Breiman, 2001) to estimate the vines' transpiration in 2021 based on the $Tv_{(obs)}$ from 2022, ecosystem fluxes and meteorological parameters. The SF_{model} was exposed to the hourly time series for the period from 01/06/2022 to 31/08/2022, using ecosystem scale latent heat (LE), sensible heat (H), global radiation (Rg), soil heat flux (G), friction velocity (u_*), VPD, air temperature (T_{air}), volumetric soil water content at 10 cm depth (usoil10), precipitation (Precip) and the mean of observed vines transpiration ($Tv_{(obs)}$) as predictors. The training was conducted using the *caret* package (Kuhn, 2008), for open-source R software (R Core Team, 2021). SF_{model} was fine-tuned using the arguments *ntree = 500, nodesize = 30, control metric = root mean square error (RMSE), bootstrapping n = 15*, (Text S4 in Supporting Information S1).

The model's performance was assessed using the leave-one-month-out cross-validation approach (for details refer to Text S4 in Supporting Information S1). The final output $Tv_{(mod)}$ is the mean of the computed Tv on each step of the cross-validation, and sd ($Tv_{(mod)}$) is the standard deviation of $Tv_{(mod)}$ obtained in a similar way. The metrics used to report the performance of SF_{model} were the generalized coefficient of determination (R^2) and the RMSE (Figure S2 in Supporting Information S1). SF_{model} was then applied to a period of the warm seasons of 2022 and 2021 (June to September) to make $Tv_{(mod)}$ available in hourly scale, which was then integrated to daily scale.

2.5. Temporal Variation in the Contribution of Components to the ET_{EC}

Combined results from the top-down and bottom-up approaches were used to obtain additional components to total ET and to define their dynamics after rainfall events.

2.5.1. Dynamics of ET Components Over Time

To understand the changes of the relative importance of each ET_{EC} component over time, a time series of transpiration fluxes in mm d^{-1} was made available for the periods June-September 2021 and June-August 2022, and including T_{EC} from partitioning ET_{EC} and $Tv_{(mod)}$ from the SF_{model}. For the same period the understorey transpiration (Tu) was estimated:

$$Tu = T_{EC} - Tv_{(mod)} \quad (5)$$

The diurnal patterns of the water fluxes' components were investigated during 9 days within the season of 2021, when besides ET_{EC} and T_{EC}, ETu fluxes were available. The selected days, 07/07/2021 (day 1), 21/07/2021 (day 2), 09/08/2021 (day 3), 10/08/2021 (day 4), 11/08/2021 (day 5), 31/08/2021 (day 6), 09/01/2021 (day 7), 21/09/2021 (day 8) and 22/09/2021 (day 9), were mainly sunny days, without rainfall and not needing more than 3 gap-filled values from 6:00 to 18:00.

2.5.2. Dynamics of ET Components From Wet to Drier Conditions

To understand the changes of the relative importance of each ET_{EC} component by increasing the time after the last rainfall event, we labeled the days within the period from 01/06/2021 to 30/09/2021 as D1 (one day after), D2 (two days after), D3 (three days after) or D3+ (more than 3 days after) according to their distance in time relative to the last day with a precipitation event, designated as D0, and selected relative fluxes of T_{EC}, Tu, $Tv_{(mod)}$ and

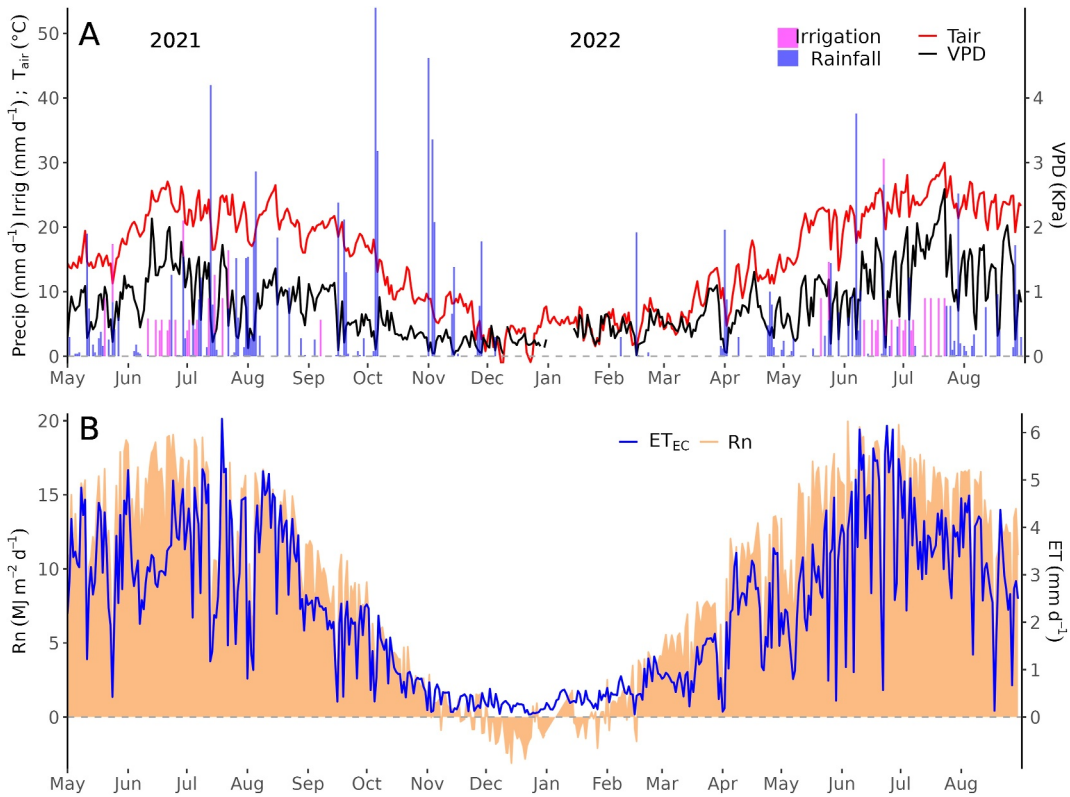

Figure 2. Temporal variability of daily mean values from May 2021 to end-August 2022 of (a) Tair (°C), vapor pressure deficit (KPa) and daily rainfall and irrigation (mm d^{-1}) and (b) Rn (MJ m^{-2} d^{-1}) and ET$_{EC}$ (mm d^{-1}) in the vineyard.

E$_{EC}$ with respect to ET$_{EC}$ (comprising at least 15 points for each component). The 9 empirical ETu values were added to the analysis as a qualitative reference. Considering ET$_{EC}$ as the sum of the T$_{EC}$ and E$_{EC}$ components, we write E$_{EC}$ as:

$$E_{EC} = ET_{EC} - T_{EC} \quad (6)$$

Then the fluxes' relative contributions were calculated by normalizing each flux by the ET$_{EC}$ on the daily scale. When calculations were performed using mean values (e.g., sums or multiplications), the resulting standard deviation was computed according to error propagation theory (Taylor, 1997).

3. Results

3.1. Meteorological Conditions

Meteorological conditions were highly variable from day-to-day (Figure 2a), as well as diurnally. Considering the daily scale, the period comprising the months from May to August had the highest Tair average (22.8 ± 3.48°C), oscillating in the range of 16.0–29.9°C. In this period the daily range for Rn was from −2.6 to 20.0 MJ m^{-2} d^{-1}, with averages of 13.7 ± 3.8 MJ m^{-2} d^{-1}. The VPD curve oscillated from 0.12 to 2.6 KPa, with a daily average of 1.06 KPa.

The precipitation was more abundant in 2021 than in the drier 2022 (May to August), as seen in the number of rain events (54 and 41 in 2021 and 2022, respectively) and cumulated water depth (348 and, 262 mm, in 2021 and 2022, respectively). However, both growing seasons had similar mean rainfall depths (6.5 ± 8.26 and 6.4 ± 8.0 mm event^{-1}, in 2021 and 2022, respectively). Despite those differences, the drip irrigation scheme proposed by the vineyard managers applied the same water depth during the mentioned period (total of 115 mm each year, distributed in 18 events within the considered time period).

19447973, 2025, 3, Downloaded from https://agupubs.onlinelibrary.wiley.com/doi/10.1029/2023WR035360 by CochraneItalia, Wiley Online Library on [28/03/2025]. See the Terms and Conditions (https://onlinelibrary.wiley.com/terms-and-conditions) on Wiley Online Library for rules of use; OA articles are governed by the applicable Creative Commons License

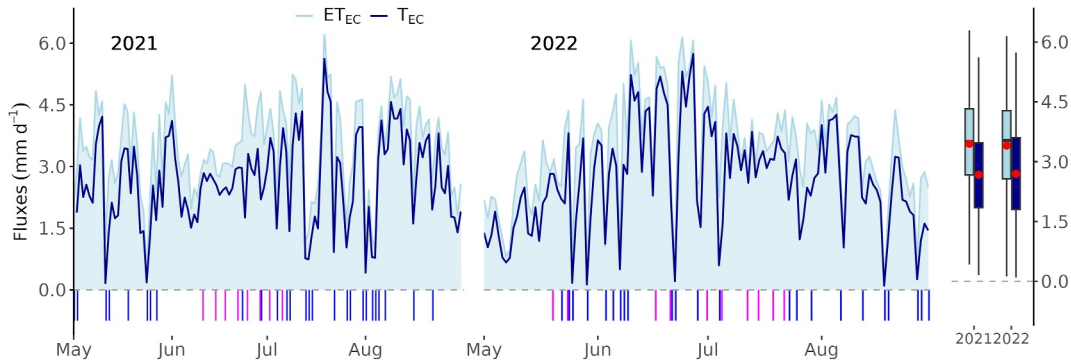

Figure 3. (left side) Temporal evolution of daily values of ET_{EC} and T_{EC} (obtained with the Transpiration Estimation Algorithm method). (right side) Boxplots showing the median, main quartiles of the distribution of the fluxes and the values range, for months from June to August. Red dots indicated mean values. The stripe plot placed below the fluxes plot indicates qualitatively the occurrence of rain or irrigation events.

3.2. ET_{EC} Partitioning (Top-Down Approach)

The growing seasons of May - August 2022 were drier and warmer. However, ET_{EC} fluxes remained similar in both years, with peaks around 5.62 mm d^{-1} in 2021 and 5.74 mm d^{-1} in 2022 (refer to Tables S10 and S11 in Supporting Information S1 for statistical tests). When comparing the fluxes on a daily scale, the mean ET_{EC} was consistent between both seasons (mean ET_{EC} of 3.45 ± 1.12 mm d^{-1} in 2021, and mean ET_{EC} of 3.40 ± 1.31 mm d^{-1} in 2022, Figure 2b).

The daily patterns of T_{EC} presented high variability, but were coherent to ET_{EC} (Figure 3) and to environmental variables such as Rn, Tair and VPD. The correlation coefficient was 0.94 between T_{EC} and ET_{EC}, and 0.82, 0.65 and 0.67 among T_{EC} and Rn, Tair and VPD, respectively (Tables S7 and S9 in Supporting Information S1). The daily mean T_{EC} was 2.68 ± 1.07 mm d^{-1} in 2021 and 2.69 ± 1.07 mm d^{-1} in 2022, representing on average 77% and 79% of ET_{EC} values in the two years respectively, as seen in the boxplots of Figure 3. By inverting Equation 1, the contribution of the ecosystem evaporation component (E_{EC}) was approximately 21%–23% of ET_{EC} in the 2021 and 2022 growing seasons.

In summary, being ET_{EC} fluxes similar in both years, the obtained T_{EC} and consequently E_{EC} also kept proportions among years (Figure 3). The T_{EC} component contributed to ~78% of the ecosystem bulk ET_{EC}.

3.3. ET Components From the EPA (Bottom-Up Approach)

3.3.1. Vines' Transpiration ($Tv_{(obs)}$ and $Tv_{(mod)}$)

The vines transpiration ($Tv_{(obs)}$) was obtained by the mean of individual $Tv_{(obs)}$ curves. Good correlations (R^2 of 0.64, 0.66, 0.84) among three $Tv_{(obs)}$ curves were observed, with a relatively low standard deviation (sd), below 0.50 mm d^{-1}, to the daily mean $Tv_{(obs)}$ (Figure S3 in Supporting Information S1). The $Tv_{(obs)}$ presented patterns with high variability, similarly to ET_{EC} and T_{EC} (Figure 4). $Tv_{(obs)}$ values from June to August were situated in the range from 0.02 to 3.67 mm d^{-1}, with mean value of 1.47 ± 0.77 mm d^{-1}, and the averaged contribution of $Tv_{(obs)}$ to ET_{EC} was 0.40 ± 0.16 mm d^{-1}. The correlation between $Tv_{(obs)}$ and ET_{EC} was moderate on a daily scale, $R^2 = 0.55$ (Table S3 in Supporting Information S1).

The vines transpiration ($Tv_{(mod)}$) for the period of June to September in 2021 and 2022 were obtained using the SF_{model}. The model's average performance obtained with the leave-One-Month-Out cross-validation method showed the R^2 of 0.61 and RMSE = 0.067 mm hr^{-1} (Figure S2 in Supporting Information S1).

From June to September, $Tv_{(mod)}$ varied in the ranges from 0.24 to 2.40 mm d^{-1} (2021) and from 0.12 to 2.50 mm d^{-1} (2022), a slightly shorter range than $Tv_{(obs)}$. The mean values of $Tv_{(mod)}$ were 1.46 ± 0.43 mm d^{-1} and 1.48 ± 0.47 mm d^{-1}, in 2021 and 2022, respectively (Figure 4).

19447973, 2025, 3, Downloaded from https://agupubs.onlinelibrary.wiley.com/doi/10.1029/2023WR035360 by CochraneItalia, Wiley Online Library on [28/03/2025]. See the Terms and Conditions (https://onlinelibrary.wiley.com/terms-and-conditions) on Wiley Online Library for rules of use; OA articles are governed by the applicable Creative Commons License

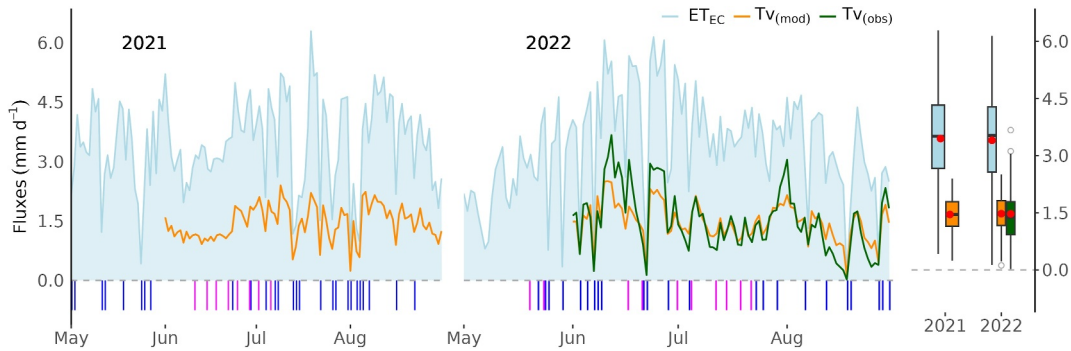

Figure 4. (left and middle) The vines' transpiration contrasted against the ecosystem reference ET_{EC}. Temporal dynamics of $Tv_{(obs)}$, $Tv_{(mod)}$ and ET_{EC} in mm d^{-1} on the left side. (right side) Boxplots showing the median, the main quartiles of the distribution of the fluxes and the values range, for months from June to August. Red dots indicated mean values. The stripe plot placed below the fluxes plot indicates qualitatively the occurrence of rain or irrigation events.

3.3.2. Understorey Evapotranspiration (ETu)

The ETu fluxes calibrated due to the tubing effect and the green leaf area per measurement spot (Texts S3.2, S3.3, and S3.4 in Supporting Information S1) in each of the five-sampling campaigns are shown in Figure 5 together with ET_{EC} to offer an ecosystem benchmark. Figure 5 also provides a reference of when rainfall occurred, classifying then the sampled days as D1, D2, D3 or D3+ according to their position in time relative to the last rainfall event. These days (referred to as chamber days, are highlighted with light blue rectangles in Figure 5) show that ET_{EC} and ETu were well correlated at hourly scale (R^2 of 0.63, Table S4 in Supporting Information S1), however their patterns differed during the days, when ETu presented higher variability and ET_{EC} looked more smoothed.

Similarly to the high variability in space and time of the total biomass of vegetation, the GLA also varied from 0.20 to 2.42 m^2 of green leaves per m^{-2} of ground surface and its mean value was 1.00 ± 0.76 m^2 m^{-2} (mean of 19 measured spots, refer to Figure S12 in Supporting Information S1).

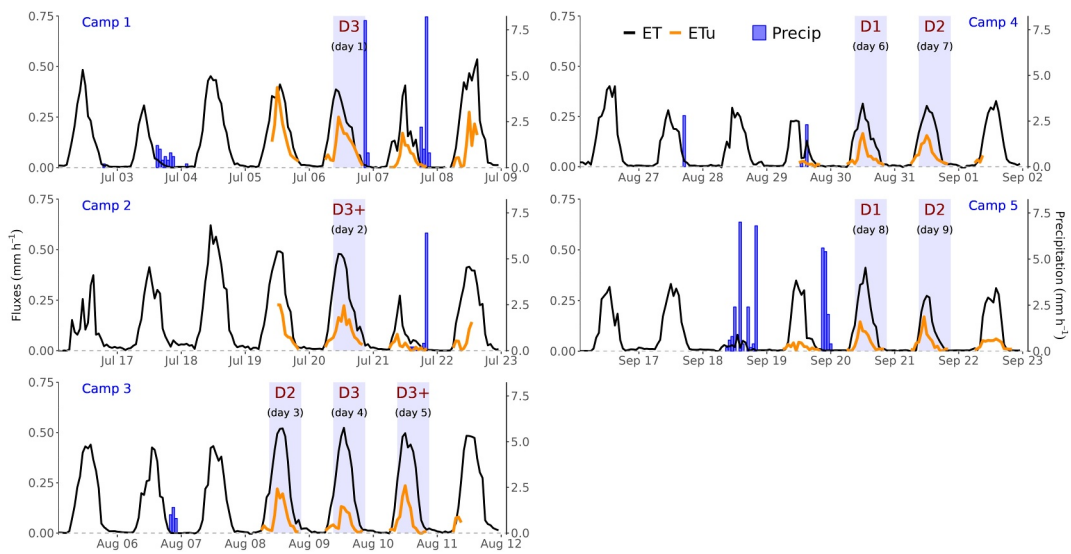

Figure 5. The five different moments of the warm season in 2021 when ETu and ET_{EC} were assessed simultaneously in the vineyard (fluxes and precipitation in mm h^{-1}). The chamber-days were highlighted with light blue rectangles, and classified as D1, D2, D3 or D3+ according to their position in time relative to the last precipitation event (days of rain are D0): 07/07/2021 (D3), 21/07/2021 (D3+), 09/08/2021 (D2), 10/08/2021 (D3), 11/08/2021 (D3+), 31/08/2021 (D1), 09/01/2021 (D2), 21/09/2021 (D1) and 22/09/2021 (D2). Data of these 9 days were included in the bottom-up approach.

19447973, 2025, 3, Downloaded from https://agupubs.onlinelibrary.wiley.com/doi/10.1029/2023WR035360 by CochraneItalia, Wiley Online Library on [28/03/2025]. See the Terms and Conditions (https://onlinelibrary.wiley.com/terms-and-conditions) on Wiley Online Library for rules of use; OA articles are governed by the applicable Creative Commons License

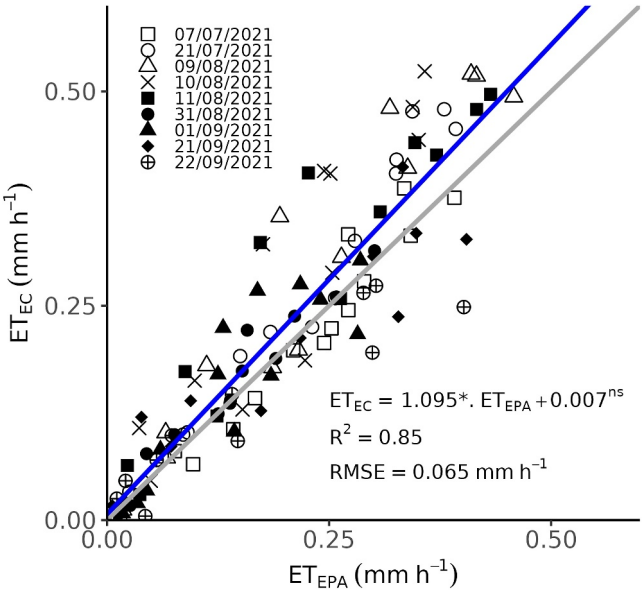

Figure 6. Agreement between the ecosystem ET_{EC} obtained with the eddy covariance method (top-down approach) and the ET_{EPA} (bottom-up approach). Points refer to hourly values for each day, the gray line indicates the identity line, and the blue line indicates the equation for the linear regression model, * stands for *p*-value <0.05, ^{ns} for *p*-value ≥0.05.

The intensities and distribution of the precipitation events also varied within campaigns, covering from Campaign 2 with no rainfall during or before 21/07/2021 to Campaign 5 with several hours of rain in the 48 hr before the days of measurements (21/09/2021 and 22/09/2021).

3.4. Agreement of the Approaches Top-Down and Bottom-Up (i.e., EPA Approach)

The comparison between the top-down and the bottom-up approaches shows a high agreement (the R^2 of the linear regression model is 0.85), and low RMSE (0.065 mm hr^{-1}, Figure 6). The slope (1.095) indicated that the total ET_{EPA} was only slightly underestimated with the bottom-up approach with respect to ET_{EC}.

3.5. Temporal Variations in the Contribution of Components to the ET_{EC}

3.5.1. Contribution of Water Flux Components to the ET_{EC}

The mean diurnal fluxes from $Tv_{(mod)}$ and ETu were displayed in Figure 7, along with ET_{EPA} and the ET_{EC} as benchmark (Figure S4 - A panel with the diurnal fluxes of the 9 days is available in Supporting Information S1). The curves show that the values of the water fluxes stayed below 0.52 mm hr^{-1} for the ET_{EC}, 0.25 mm hr^{-1} for the ETu and 0.26 mm hr^{-1} for the $Tv_{(mod)}$. It can be observed that the three fluxes have distinct patterns during the days: while ET_{EC} showed the expected bell-shaped curve in all the (sunny) days with the exception of the (partially cloudy) day 9, ETu presented a more unstable behavior in shape and intensity, with peaks generally happening later in the day with respect to ET_{EC}. $Tv_{(mod)}$ presented instead a pattern more closely correlated to ET_{EC} and more responsive to the meteorological variables measured above the canopy, such as to Rn (R^2 of 0.92).

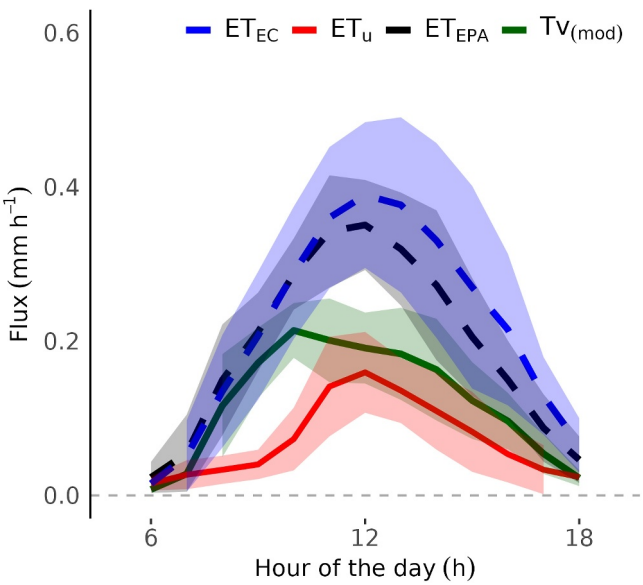

Figure 7. Diurnal patterns of ET_{EC}, ET_{EPA} (solid lines), ETu and $Tv_{(mod)}$ (dashed lines) fluxes in mm h^{-1} averaged over the 9 days using the ground flux chambers, and the fluxes' respective standard deviations (shaded bands). The bottom-up ecosystem ET (ET_{EPA}) matches well ET_{EC} (the Eddy Covariance obtained ecosystem ET), mainly in the morning hours, during which the fluxes are dominated by the grapevines ($Tv_{(mod)}$). The understorey component (ETu) peaked later in the day, around noon.

ET from the bottom-up approach (ET_{EPA}) showed a similar pattern to ET_{EC} (line plots in Figure 7), and the magnitudes were also similar during the course of the day (average of peak values of 0.46 mm hr^{-1} and 0.52 mm hr^{-1} around midday, for ET_{EPA} and ET_{EC}, respectively).

The ratios corresponding to the relative contributions of $Tv_{(mod)}$, T_u and T_{EC} to the ET_{EC} did not show smoothed nor clear seasonal patterns when compared to the absolute fluxes of $Tv_{(mod)}$, T_u and T_{EC}, maintaining a high daily variability over the warm seasons of 2021 and 2022 (i.e., from May to September), in Figure 8.

The boxplot analysis pointed to high T_{EC} contribution, dominating the ecosystem ET (Figure 8), while $Tv_{(mod)}$ and T_u have similar median values. The understorey contribution had lower mean values (0.30 ± 0.17 to 0.37 ± 0.22 in 2021 and 2022, respectively) when compared to the vines', however T_u/ET_{EC} had wider ranges encompassing near-zero values. The mean T_{EC} contribution to ET_{EC} (0.76 ± 0.13 to 0.79 ± 0.16) was in general higher than the individual contribution of the vines or the understorey, as expected.

3.5.2. Source Contributions to ET From Wet to Drier Conditions

The relative contribution of the flux components changed with time after precipitation. Considering the averaged values, the non-linear responses showed that T_{EC}/ET_{EC} increased from 0.69 to 0.86 moving from D1 to D3+, indicating the dominance of the ecosystem transpiration over the ecosystem

19447973, 2025, 3, Downloaded from https://agupubs.onlinelibrary.wiley.com/doi/10.1029/2023WR035360 by CochraneItalia, Wiley Online Library on [28/03/2025]. See the Terms and Conditions (https://onlinelibrary.wiley.com/terms-and-conditions) on Wiley Online Library for rules of use; OA articles are governed by the applicable Creative Commons License

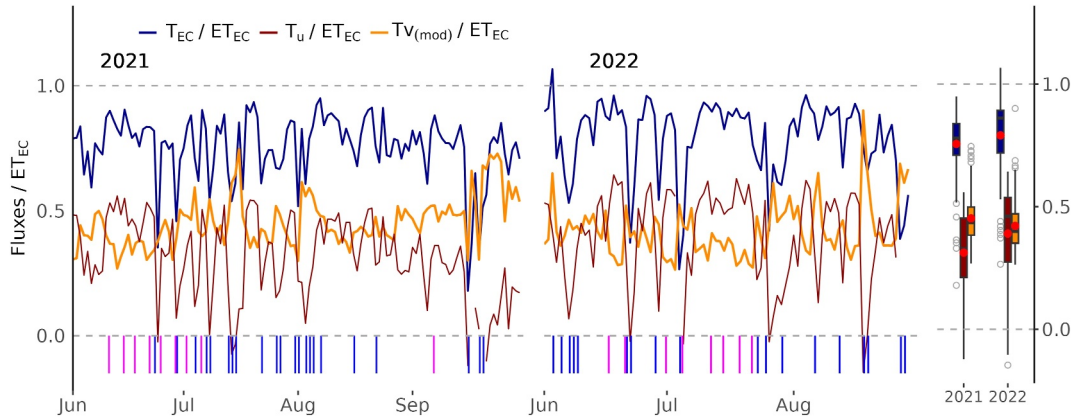

Figure 8. Relative contributions of $Tv_{(mod)}$, T_u and T_{EC} to the ET_{EC} over the warm seasons of 2021 and 2022 (months from June to September). Boxplots showing the median, the main quartiles of the distribution of the fluxes and the values range for the same months of the two seasons. Red dots indicated mean values. The stripe plot placed below the fluxes plot indicates qualitatively the occurrence of rain or irrigation events.

evaporation (E_{EC}), which makes sense when the surfaces are no longer wet. In this way, the E_{EC}/ET_{EC} decreased from 0.31 to 0.14 (from D1 to D3+, Figure 9).

From the vines component, their transpiration ($Tv_{(mod)}/ET_{EC}$) decreased from 0.49 to 0.37 as the system moved into drier days (i.e., toward D3+), as long as the proportion of the understorey contribution (Tu/ET) increased. From this we may infer that the understorey vegetation could have a more efficient use of water in dry moments,

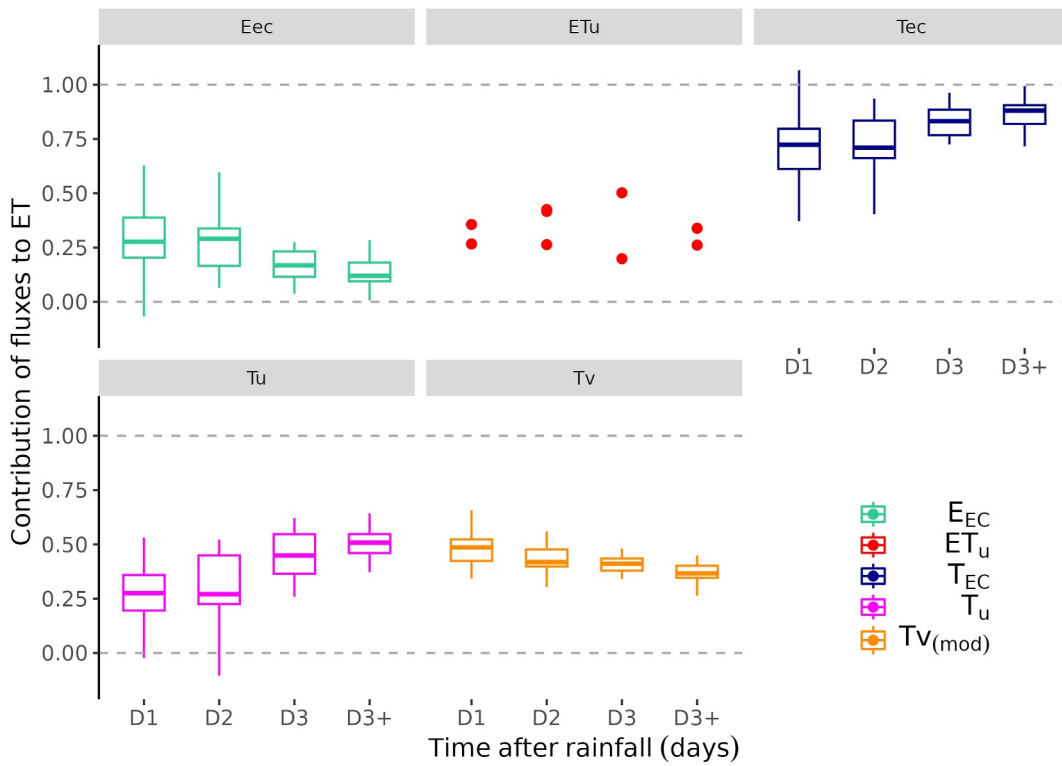

Figure 9. Relative fluxes of ETu, T_{EC}, Tu, $Tv_{(mod)}$, E_{EC} with respect to ET_{EC} (mm d^{-1}/mm d^{-1}) in sequential days after precipitation (D1 to D3+). The data used in this analysis are daily fluxes from 01/05/2021 to 31/08/2022 of T_{EC}, Tu, $Tv_{(mod)}$, E_{EC}, and the ETu from the 9 days of chamber data. The patterns show how the relative contribution to the ET_{EC} of each component evolves from wet moments to drier conditions. Boxplots show the median, the main quartiles of the distribution of the fluxes and the values ranges each day after rainfall.

19447973, 2025, 3, Downloaded from https://agupubs.onlinelibrary.wiley.com/doi/10.1029/2023WR035360 by CochraneItalia, Wiley Online Library on [28/03/2025]. See the Terms and Conditions (https://onlinelibrary.wiley.com/terms-and-conditions) on Wiley Online Library for rules of use; OA articles are governed by the applicable Creative Commons License

19447973, 2025, 3, Downloaded from https://agupubs.onlinelibrary.wiley.com/doi/10.1029/2023WR035360 by CochraneItalia, Wiley Online Library on [28/03/2025]. See the Terms and Conditions (https://onlinelibrary.wiley.com/terms-and-conditions) on Wiley Online Library for rules of use; OA articles are governed by the applicable Creative Commons License

and it suggests that the irrigation is important for the vines. The ETu/ET_{EC} values also varied within a short range (0.50–0.20), suggesting that the contribution from the bulk understorey component would not increase after 3 days after rainfall, while the understorey transpiration contribution (Tu/ET_{EC}, from 0.24 to 0.50, D1 to D3+) explains the increase in T_{EC}/ET_{EC} in combination with the slightly decreasing $Tv_{(mod)}/ET_{EC}$.

4. Discussion

4.1. ET_{EC} Partitioning (Top-Down Approach)

The top-down approach was adopted to assess the fractional contribution of total transpiration processes to ecosystem evapotranspiration (objective 1).

Eddy Covariance is usually considered a reliable method and taken as a reference to compare alternative methods against. Nevertheless, its measurements are associated with errors that may be due to, for instance, to the spatial variability of the footprint area, the data processing and gap-filling steps (Papale et al., 2006), and to micro-meteorological issues, which is the case of the imperfect energy balance closure (Foken, 2008). In our study, the sonic anemometer, gas analyzer and the radiometer were placed 3.0–4.0 m above the vines' canopy to reduce the interference of agricultural spray treatments on the sensors, at the cost of a slight increase at the edge of the footprint (on average the vineyard represents 90% of the footprint). Furthermore, the neighboring areas are composed of vineyards and the bias due to those are expected to be minimal.

The data processing and gap-filling steps followed the most frequently used protocols in literature (Reichstein et al., 2005), performed using the ReddyProcWeb online tool described by Wutzler et al., 2018 (https://bgc.iwww.mpg.de/5622399/REddyProc). Moreover, a well-established and balanced method for the closure of the energy balance (#4 reported by Wohlfahrt et al., 2009) was applied, correcting for the energy unbalance in monthly intervals, given the energy imbalance tends to improve as the averaging time is increased (Finnigan et al., 2003; Grachev et al., 2020; Mauder & Foken, 2006). This approach matches our work context since most of the analysis we did included two consecutive years' warm seasons. A brief comparison between monthly and daily time intervals is available (Figure S5 in Supporting Information S1).

In the months from June to September of both seasons, values of the EBR ranged from 0.77 to 1.02 (0.89 ± 0.08, mean ± sd), indicating that turbulent fluxes were on average 11% lower than the available energy. This value is similar to other works in vineyards: 0.86–1.01 (Jiao et al., 2018), 0.91 (Kool et al., 2016), 0.88 (Poblete-Echeverría & Ortega-Farias, 2013), and in agreement with other studies reporting a lack of closure in the energy balance between 10% and 30% (Foken, 2008; Stoy et al., 2013; Wilson et al., 2002). The ET_{EC} after EBC corrections also stayed within a plausible range for vineyards, from June to September: 4.8–5.4 mm d^{-1} for our site, 2.6–5.7 mm d^{-1} for literature (Ferreira et al., 2012; Kool et al., 2016; Poblete-Echeverría & Ortega-Farias, 2013; Zhang et al., 2011; Zhao, Kang, et al., 2018).

The high variability shown in the ET_{EC} patterns indicate the fast response of the water fluxes to environmental drivers (e.g., Rn, Tair) (Montagnani et al., 2018), that can change in short time periods, often within few hours or from day-to-day, especially in areas surrounded by mountains as our site (Wenter et al., 2018; Zanotelli et al., 2019). In fact, the correlation coefficients between $ET_{EC} \sim Rn$ and $ET_{EC} \sim Tair$ were high (0.88 and 0.69 - Table S5 in Supporting Information S1). Some periods with transpiration approximately equaling ET_{EC} could be graphically identified as dry periods (i.e., dry spells). Such moments coincide with periods without rainfall, for instance in June 2021 and July 2022, when Rn was available, Tair was high while ET_{EC} decreased.

The TEA method for transpiration estimation (Nelson et al., 2018) was previously used in croplands, such as winter wheat, barley and summer maize, and in forests (Hu & Lei, 2021; Paul-Limoges et al., 2020, 2022). As far as we know, the present study is the first attempt to apply it to partition ET from a grassed vineyard. In the studies with the cereal monocultures and crop rotations, the T/ET ratio was believed to be overestimated, when compared to other models. This was attributed to the effect of less vegetated or less dense canopy on the TEA algorithm. Since TEA's main assumption is that the maximum T/ET reaches unity when upper soil layers are dry, less vegetated areas might have small WUE_{eco}, hence the ET_{EC} partitioning is likely to not perform so well (Paul-Limoges et al., 2022). In contrast with the annual croplands, TEA performed well in systems as forests with full canopy closures (e.g., Paul-Limoges et al., 2020). The site described in this study more closely resembled the latter, since the vineyard's understorey strongly present from early spring to late fall, and the vines' canopies were in full development during the study period.

19447973, 2025, 3, Downloaded from https://agupubs.onlinelibrary.wiley.com/doi/10.1029/2023WR035360 by CochraneItalia, Wiley Online Library on [28/03/2025]. See the Terms and Conditions (https://onlinelibrary.wiley.com/terms-and-conditions) on Wiley Online Library for rules of use; OA articles are governed by the applicable Creative Commons License

Slightly lower T/ET ratios were reported in other studies compared to ours, such as 0.60 for grasslands, 0.56 for evergreen needle leaf forests (Zhou et al., 2016), 0.64–0.70 for rice (Hossen et al., 2012), 0.60–0.70 for corn, wheat, and soybean (Kool et al., 2014). Irrigated vineyards had T/ET in the range of 0.52–0.87 (Ferreira et al., 2012; Poblete-Echeverría & Ortega-Farias, 2013; Trambouze et al., 1998; Zhang et al., 2011).

During most of the season, T_{EC} dominated ET_{EC}, while E provided a considerably lower contribution despite the several rainfall events. These events lowered T_{EC} during a few days, coherently with a significant decrease in daily Rn and Tair values (Figure 2), but T_{EC}/ET_{EC} showed a fast recovery as soon as the typical summer conditions were back. The top-down approach allowed us to achieve the first objective of this paper, attributing to overall transpiration processes 77% and 79% of total ET_{EC} in 2021 and 2022, respectively. Considering the soil texture and the large presence of stones, it is very likely that the water supplied by the drip irrigation system was unavailable for the understorey vegetation in the alleys where it also could not fuel the E process while it boosted the transpiration of both vines and understorey vegetation growing along the vine row. The TEA partitioning results are consistent with other models across ecosystem functional types (Hu & Lei, 2021; Li et al., 2019; Nelson et al., 2020; Scott et al., 2021; Yu, Zhou, et al., 2022, Yu, Zhou, et al., 2022), however, as any model can introduce uncertainty, data interpretation should be done with caution.

4.2. ET Components From the EPA (Bottom-Up Approach)

The bottom-up approach was applied to answer the question about the relative contribution of the vines and the understorey vegetation transpiration fluxes to the total ET and T fluxes (objective 2).

We opted to upscale our $Tv_{(obs)}$ results to ecosystem scale to support the comparison against the other water vapor sources in the scale of the vineyard. Among the monitored variables, Tair, Rn and VPD were able to partially explain the high variability in the $Tv_{(obs)}$ time series (linear regression R^2 of 0.03, 0.37, 0.03, respectively), and were the main drivers of ecosystem scale fluxes (i.e., ET_{EC}, T_{EC}). Among the main drivers of Tv, the Rn and VPD had relevant correlation in a Chinese vineyard (Zhang et al., 2016), which contrasted our site where the conditions provided a time lag between $Tv_{(obs)}$ and Tair, resulting in the lack of correlation with VPD.

Similar seasonal trends with high variability among days were reported in different land use types such as a mixed forest (Paul-Limoges et al., 2020), wheat (Rafi et al., 2019) and in a vineyard (Gao et al., 2019). This behavior reflects how fast the vegetation reacts to environmental stimuli (in ecosystem scale). The averaged $Tv_{(obs)}$ diurnal patterns also agreed with the reported ones obtained using sap flow sensors in apple plants (Ben Abdelkader et al., 2022), potted grapevines plants (Benyahia et al., 2023) and vineyard (Zhang et al., 2011), as well as measured with other methods in grapevine growing in controlled conditions (Shtai et al., 2024).

Modeling Tv curves in response to the environmental conditions made it possible to estimate the Tv flux in the first of the 2 years using data from the second year, and work on the hydrological balance. Machine learning approaches are efficient in capturing patterns and insights from complex data (Reichstein et al., 2019), and among them the random forest structure is effective in assessing relations between independent and dependent variables, linear or not (Nelson et al., 2018; Yu, Orth, et al., 2022). The modeled vine transpiration time series agreed with the decreasing pattern of ET_{EC} in dry periods also characterized by non-optimal Tair conditions. Moreover, during the particularly dry month of July 2022, both $Tv_{(mod)}$ and $Tv_{(obs)}$ decreased in range of values, emphasizing the ability of the SF_{model} in capturing the Tv dynamics.

As is often done when using the chambers method (Simpson et al., 2019; Varolo et al., 2016), the assessment of understorey fluxes was limited to short campaigns over the warm season to cope with issues related to both spatial representativeness and logistics in the field management. The low performances of the chamber's method under low VPD (Cui et al., 2020; Simpson et al., 2019) was dealt with by removing night time values and filtering the data by coefficient of determinations of the linear model (threshold set at $R^2 > 0.80$, which contributed to eliminating values from when the relative humidity were above 90%). The effect of sorption and desorption of water vapor in tubes was addressed in some Eddy covariance studies (Ibrom et al., 2007; Nordbo et al., 2013; Runkle et al., 2012; Zhang et al., 2023) but very few studies have addressed this issue for the chamber's method. Simpson et al. (2019), who adopted a similar approach to ours, reported a comparison between the fluxes obtained using 1-m and 10-m-long tubes, and the ratio of 1 m/10 m was ~2.0, which was used as a correction factor. Our ratio (of 1.76) obtained with another calibration approach applying the same devices and tubing used in the field,

19447973, 2025, 3, Downloaded from https://agupubs.onlinelibrary.wiley.com/doi/10.1029/2023WR035360 by CochraneItalia, Wiley Online Library on [28/03/2025]. See the Terms and Conditions (https://onlinelibrary.wiley.com/terms-and-conditions) on Wiley Online Library for rules of use; OA articles are governed by the applicable Creative Commons License

was of similar magnitude, and confirmed the expected underestimation of the ETu fluxes due tube attenuation effect. A third issue with regards to chamber method is linked with the vegetation height. The previous works usually focused on measuring fluxes from low vegetation or bare soil (Raz-Yaseef et al., 2010; Varolo et al., 2016) while in our site, some grass species had vigorous growth and were taller than 20 cm, hampering the proper closure of the chamber's dome. The applied solution of upscaling the fluxes obtained from the $GLA_{<10\ cm}$ portion of the vegetation to the whole understorey vegetation worked as a scalar multiplier that took into account the vertical distribution of the GLA. This procedure offers the advantage of being collar-specific thus allowing to take into account the spatial heterogeneity of the site.

On the other hand, upscaling ETu based on GLA is prone to uncertainty due to two main factors: (a) when plants are cut to fit in the chamber the plant physiology can be impacted, similarly to how any disturbances in ecosystems can affect the transpiration dynamics, also seen when grazing in wheat fields introduced a high variation on T/ET (Raghav et al., 2022); (b) although the E contribution (from the soil and understorey vegetation surface) itself cannot be estimated in this setup, it is not assumed to be negligible at the ground level. In fact, it results that multiplying initial ETu by $(GLA_{>10\ cm} + GLA_{<10\ cm})/GLA_{<10\ cm}$ for each collar actually upscales both E and Tu components.

The daily integrals of ETu in the nine selected campaign days were within 0.62 and 1.52 mm d^{-1}, always lower with respect to Tv. The diurnal patterns of water fluxes in the vineyard showed that the ETu component increased later than the $Tv_{(mod)}$, and their peaks were not synchronised (Figure 7). This result was also reported by Paul-Limoges et al. (2020) when investigating above- and below-canopy ET fluxes in a forest of deciduous trees. The lack of coordination between different portions of the ecosystem is likely the result of the different micrometeorological conditions, which in hedgerow cropland may affect radiation availability, relative humidity, and temperature (Tezza et al., 2019). Qubaja et al. (2020) reported similar patterns, with a difference that in their semi-arid *Pinus halepensis* forest environment the understorey component was composed only of soil evaporation. Additionally, in this study, we found high agreement between the eddy measured ET_{EC} hourly values and ET obtained by summing $Tv_{(mod)}$ and ETu (bottom up approach) at the same time scales The good correlation coefficient ($R^2 = 0.85$ of a linear regression model, Figure 6) supports the consistency of the adopted methodology and is in accordance with other works that applied similar approaches in different land use types, although reporting data at a daily time scale: for example, Soubie et al. (2016) ($R^2 = 0.55$–0.61, in mixed temperate forest, $n > 200$), Qubaja et al. (2020) ($R^2 = 0.98$, in dry pine forest, $n > 11$) and Zhao et al. (2015) ($R^2 = 0.87$–0.89, in a vineyard of northwest China, $n = 18$). The intercept of the linear model is not significantly different from zero, meaning there is no offset between the approaches, and the slope shows that ET_{EPA} slightly underestimated the ET_{EC} ($ET_{EC} = 1.104^{*}\ ET_{EPA} + 0.0006^{ns}$). The EPA approach was applied at this vineyard considering the additive model $ET_{EPA} = Tv_{(mod)} + ETu$, with the assumption that the evaporation of the vines' canopies Ev was negligible. Although considering Ev negligible can lead to considerable discrepancies (Stoy et al., 2019), it was necessary given the difficulties to obtain quantitative meaningful information in the experimental context. This possibly caused ET_{EPA} underestimation in our results, even though it is not an unusual assumption, made by several models for ET partitioning (Paul-Limoges et al., 2020), especially in systems like ours with sparse canopies. Studies have found that rainfall interception does not greatly affect ET partitioning results (Tong et al., 2019), even when distinguishing between two vegetation types in a tree-grass ecosystem (Cui et al., 2024). Furthermore, the data used in the Bottom-up approach combines $Tv_{(mod)} + ETu$ coming from the 9 selected days (Figure S4 in Supporting Information S1), which were days without rainfall, and the vines canopy were expected to be dry, minimizing possible bias related to this assumption.

Based on the results from both bottom-up and top-down approaches, we can state that vines had a slightly higher contribution on total ecosystem transpiration with respect to understorey vegetation, representing on average 45% and 42% of it in 2021 and 2022 respectively (in contrast to the understorey contribution of 30% and 37% per year). The partial contribution of the understorey to total T and ET was higher in the dryer 2022 season and increased with the days from last rainfall. These results agree with the increased exchange of latent heat occurring during dry periods reported for different European grasslands by Teuling et al. (2010), suggesting a less conservative behavior of grassland in the use of water resources in comparison to forests, at least for the initial period of stress development.

19447973, 2025, 3, Downloaded from https://agupubs.onlinelibrary.wiley.com/doi/10.1029/2023WR035360 by CochraneItalia, Wiley Online Library on [28/03/2025]. See the Terms and Conditions (https://onlinelibrary.wiley.com/terms-and-conditions) on Wiley Online Library for rules of use; OA articles are governed by the applicable Creative Commons License

4.3. Temporal Variations in the Contribution of Components to the ET_{EC}

Grouping the different water fluxes based on their distance from the last rainfall event, allowed us to show their relative importance on total ET_{EC} in the first 3 days following a rain event. The ecosystem transpiration showed a clear increasing tendency, passing from 0.74 on the first day after rain and reaching 0.83 in approximately 72 hr. As vine transpiration slightly decreased within the range of 0.54–0.45, without a strong tendency, we therefore speculated that the understorey transpiration increased once the system got drier, contributing to the increasing T_{EC}.

In addition to the known strong increase in transpiration of grassland under high temperatures (Teuling et al., 2010), the different patterns of $Tv_{(mod)}$ and Tu could be partially explained also by the use of drip irrigation. The irrigation days were not removed from the analyzed data, as they were considered part of the agroecosystem environment and the portion of input water returning to the atmosphere would be reflected in ET_{EC} fluxes assessed with our sensors. The vines were thus not exposed to any periods of severe drought, being able to keep their transpiration values in the aforementioned range, with only moderate changes. The portion of the understorey vegetation that accessed irrigation water was only a narrow strip below the vine's canopies (roughly 35% of the vineyard floor). Together with the fact that the understorey vegetation had relatively short roots, in comparison with the vines' (Callesen et al., 2023), it can be concluded that the understorey portion was subjected to drought conditions, and rainfall enhanced Tu. In this analysis, the implicit competition among multiple plant species for access to both above and below-ground available water is considered. This observed pattern, along with the predominance of Transpiration (T) over Evapotranspiration (ET_{EC}) in grasslands with high Leaf Area Index (>2), aligns with findings from other recent partitioning studies conducted at the global level (Burchard-Levine et al., 2022; Wei et al., 2017).

Despite having limited ETu data points, a decreasing tendency starts to be noticed once the ecosystem moves toward drier conditions. On average, ETu represented approximately 34% of the contribution to ET_{EC}. It makes sense that, since Tu increased with time after precipitation, the ecosystem Evaporation (E_{EC}) decreased. The points in Figure 9 show a scattered distribution for ETu/ET_{EC} especially from D2 on. The spread ETu values derive from the heterogeneity found in the understorey portion, as ETu is the average of values assessed in representative spots, spanning over irrigated portions and the rainfed interrows.

The variations in precipitation influence ETu measurements and have significant implications for the study. Rainfall increases free water in the system, leading to heightened E and T rates, consequently resulting in higher ETu values immediately following rain events. Also, the amount of rainwater influences ETu since the effects of "light" rainfall may be minimal on Tu measurements if water does not infiltrate into the soil. These conditions can skew measurements and affect the reliability of the results. Post-rain ETu patterns are expected to decrease as the system dries and evaporation rates decline, highlighting the sensitivity of ETu values to rainfall.

4.4. Applicability of This Work

While the literature has mainly focused on the partitioning of evapotranspiration into soil evaporation and plant transpiration (Kool et al., 2014; Zhang et al., 2011), the main strength of this study is that it represents one of the few attempts to separate the transpiration of grapevines from that of the herbaceous vegetation growing in the vineyard alleys. Being able to distinguish between their contribution along the season has important practical implications, considering that localized irrigation systems affect water availability of grapevines only, while the transpiration of the herbaceous vegetation growing on the vineyard floor relies mainly on water from rain. To the best of our knowledge, only Cui et al. (2024), while our study was undergoing, attempted to separate the transpiration of kiwifruit vines from that of the understorey vegetation under a warm and humid climate and with plants irrigated by sprinklers. In their study, carried out in a commercial orchard, the density of understorey vegetation was, however, relatively low due to the frequent use of herbicides and mechanical tillage. The significance of the findings of this study, that included both a top-down and a bottom-up approach, experimental data and modeling, are not limited to grapevines, which is one of the most important crops in Mediterranean areas, but also apply to other sparsely vegetated areas like some agroforestry systems, row crops and orchards.

19447973, 2025, 3, Downloaded from https://agupubs.onlinelibrary.wiley.com/doi/10.1029/2023WR035360 by CochraneItalia, Wiley Online Library on [28/03/2025]. See the Terms and Conditions (https://onlinelibrary.wiley.com/terms-and-conditions) on Wiley Online Library for rules of use; OA articles are governed by the applicable Creative Commons License

5. Toward Better Measurements of Ecosystem Transpiration

Transpiration is of high importance to the global terrestrial ET (Wei et al., 2017). The impact of climate changes on biomes, including the specificities and micrometeorological drivers influencing complex physiological responses, remains uncertain. As Krich et al. (2022) suggested, the coupling of leaf-level photosynthesis and stomatal conductance may need re-examination. It is unclear whether the role of ecosystem transpiration will change, leading to stomatal closure to reduce water losses or an increase in the atmosphere's capacity to hold water vapor (Paul-Limoges et al., 2020).

In the context that temperature is expected to increase and more extreme droughts to occur (IPCC, 2023), overall levels of drought and heat stress (Asensio et al., 2022) in combination to effects due agricultural management (Callesen et al., 2023) are yet not fully understood and described by carbon and water ecosystem flux models. Specifically in the case of flux partitioning in a multi-layer ecosystem (Cui et al., 2024), such as this work's vineyard.

In this scenario, there is an apparent need to improve data collection and models. One way to achieve better flux estimates is through more accurate and specific data collection methods. Recommendations arising from the present work include:

1. Employing larger chambers capable of encompassing the entire mass of understorey vegetation, eliminating the need to cut vegetation for chamber dome closure during measurements.
2. Conducting a calibration of chamber water fluxes against weighting cells, considering not only weights and cumulative fluxes but also temperature and relative humidity. Investigating potential response lags between understorey and above-canopy fluxes is essential.
3. ET partitioning models can benefit from data collected from distinct layers. For example, measuring micrometeorological variables both above-canopies and understorey is essential, so it is recommended to assess at least air temperature, relative humidity and solar radiation (preferably at several points to account for canopy shadowing effects). Additionally, estimating leaf area (LA) with some frequency (e.g., monthly) is crucial to incorporate phenological inputs.

6. Conclusions

Our findings underscore the significant variability in ET and transpiration fluxes driven by fluctuating meteorological conditions, particularly VPD, net radiation (Rn), and air temperature (Tair).

Even in highly variable environmental conditions, the biologically mediated transpiration process represented the major water flux occurring in the agroecosystem, with the ecosystem T/ET fraction consistently high, ranging from 0.77 in the wetter 2021 summer to 0.79 in the drier 2022 (estimated by the TEA in the top-down approach). This conclusion is further supported by our analysis of water fluxes after a rainfall, where T/ET increased from 0.69 to 0.86 between the first and third days after rainfall.

The bottom-up approach indicated that the vines are the primary contributors to ecosystem ET, especially under wet conditions, contributing 0.49 and 0.37 in 2021 and 2022, respectively. As the system becomes drier, the understorey's contribution to transpiration increases significantly, with its fraction rising from 0.24 to 0.50 between 2021 and 2022.

We also observed that the ecosystem Evaporation reached its maximum in the first day after a rain event, accounting for 0.31 of ET, but its relative contribution decreased as the system dried out.

Ultimately, this is among the first studies to provide a detailed quantification of the T/ET ratio in the complex multi-layered agro-ecosystem of a grassed vineyard, and to separate the contributions of vines and understorey vegetation to the bulk water vapor dynamics. Considering the increasing trend of including agroecological measures such as cover crops, to improve the sustainability and resilience of the perennial crop plantations and the concurrent context of reduced water availability foreseen in the future, these findings are relevant for a better quantification of their water needs and proper adaptation of orchard and vineyard management.

Data Availability Statement

The data used in this study is available at https://doi.org/10.5281/zenodo.10498242 (data for the main analysis) and https://doi.org/10.5281/zenodo.10863881 (data set for the SF_{model}). Code for the TEA method is available at https://github.com/jnelson18/ecosystem-transpiration. Apart from it, all scripts used were developed in R, and are available at https://github.com/flaviobastoscampos/SFmodel_Plt (code for the SF_{model}) https://github.com/flaviobastoscampos/ET_dynamics_and_partitioning_vineyard (code to reproduce the figures).

Acknowledgments
We thank Dr. Nuno Carvalhais for his valuable contribution in time series analysis. This study was supported by the following projects: WAVE (Water losses and carbon assimilation in the vineyard as affected by changes of environmental drivers; TN 201E) project (Internal project Free University of Bolzano-Bozen); CLEVAS (Effect of climate extremes on grapevine production in South Tyrol: early detection of abiotic stress and consequences for wine quality) project (funded by the Autonomous Province of Bolzano-Bozen), and the Agritech National Research Center and received funding from the European Union Next-Generation EU (PIANO NAZIONALE DI RIPRESA E RESILIENZA (PNRR)—MISSIONE 4 COMPONENTE 2, INVESTIMENTO 1.4—D.D. 1032 17/06/2022, CN00000022). This manuscript reflects only the authors' views and opinions, neither the European Union nor the European Commission can be considered responsible for them. We are grateful to the editors and the anonymous reviewers for all the insightful comments on the paper.

References

Abdalla, M., Hastings, A., Cheng, K., Yue, Q., Chadwick, D., Espenberg, M., et al. (2019). A critical review of the impacts of cover crops on nitrogen leaching, net greenhouse gas balance and crop productivity. *Global Change Biology*, *25*(8), 2530–2543. https://doi.org/10.1111/gcb.14644

Alam, M. S., Lamb, D. W., & Warwick, N. W. M. (2021). A canopy transpiration model based on scaling up stomatal conductance and radiation interception as affected by leaf area index. *Water*, *13*(3), 252. https://doi.org/10.3390/w13030252

Allen, R. G., Pereira, L. S., Raes, D., & Smith, M. (1998). FAO irrigation and drainage paper no. 56.

Asensio, D., Shtai, W., Kadison, A., Schwarz, M., Hoellrigl, J., Steiner, M., et al. (2022). Interactive effects of high temperatures and drought on grapevine physiology during a simulated heat wave. EGU General Assembly 2022, Vienna, Austria, 23-27 May 2022, EGU22-3171. https://doi.org/10.5194/egusphere-egu22-3171

Baldocchi, D. D., Hincks, B. B., & Meyers, T. P. (1988). Measuring biosphere-atmosphere exchanges of biologically related gases with micrometeorological methods. *Ecology*, *69*(5), 1331–1340. https://doi.org/10.2307/1941631

Bambach, N., Kustas, W., Alfieri, J., Prueger, J., Hipps, L., McKee, L., et al. (2022). Evapotranspiration uncertainty at micrometeorological scales: The impact of the eddy covariance energy imbalance and correction methods. *Irrigation Science*, *40*(4–5), 445–461. https://doi.org/10.1007/s00271-022-00783-1

Ben Abdelkader, A., Benyahia, F., Bastos Campos, F., Asensio, D., Andreotti, C., Tagliavini, M., et al. (2022). Apple tree transpiration during cycles of progressive drought as assessed via continuous gravimetric and xylem sap flux measurements. *Italus Hortus*, *29*(2), 35–46. https://doi.org/10.26353/j.itahort/2022.2.3546

Benyahia, F., Bastos Campos, F., Abdelkader Ben, A., et al. (2023). Assessing grapevine water status by integrating vine transpiration, leaf gas exchanges, chlorophyll fluorescence and sap flow measurements. 1–17.

Breiman. (2001). Random forests. *Machine Learning*, *45*, 5–32.

Burba, G. (2013). Eddy covariance method-for scientific. *Industrial, Agricultural, and Regulatory Applications*.

Burchard-Levine, V., Nieto, H., Riaño, D., Kustas, W. P., Migliavacca, M., El-Madany, T. S., et al. (2022). A remote sensing-based three-source energy balance model to improve global estimations of evapotranspiration in semi-arid tree-grass ecosystems. *Global Change Biology*, *28*(4), 1493–1515. https://doi.org/10.1111/gcb.16002

Callesen, T. O., Gonzalez, C. V., Bastos Campos, F., Zanotelli, D., Tagliavini, M., & Montagnani, L. (2023). Understanding carbon sequestration, allocation, and ecosystem storage in a grassed vineyard. *Geoderma Regional*, *34*, e00674. https://doi.org/10.1016/j.geodrs.2023.e00674

Cohen, L. R., Raz-Yaseef, N., Curtis, J. B., Young, J. M., Rahn, T. A., Wilson, C. J., et al. (2015). Measuring diurnal cycles of evapotranspiration in the Arctic with an automated chamber system. *Ecohydrology*, *8*(4), 652–659. https://doi.org/10.1002/eco.1532

Cui, J., Tian, L., Wei, Z., Huntingford, C., Wang, P., Cai, Z., et al. (2020). Quantifying the controls on evapotranspiration partitioning in the highest alpine meadow ecosystem. *Water Resources Research*, *56*(4). https://doi.org/10.1029/2019WR024815

Cui, N., Zheng, S., Jiang, S., Wang, M., Zhao, L., He, Z., et al. (2024). Evapotranspiration partitioning based on underlying conductance in a complex tree-grass orchard ecosystem in the humid area of southern China. *Agricultural and Forest Meteorology*, *344*, 109796. https://doi.org/10.1016/j.agrformet.2023.109796

De Hertog, S. J., Lopez-Fabara, C. E., van der Ent, R., Keune, J., Miralles, D. G., Portmann, R., et al. (2023). Effects of idealised land cover and land management changes on the atmospheric water cycle. *Earth System Dynamics*, *14*(3), 629–667. https://doi.org/10.5194/egusphere-2023-953

Duursma, R. A., & Medlyn, B. E. (2012). MAESPA: A model to study interactions between water limitation, environmental drivers and vegetation function at tree and stand levels, with an example application to [CO2] × drought interactions. *Geoscientific Model Development*, *5*(4), 919–940. https://doi.org/10.5194/gmd-5-919-2012

FAO. (2016). Area equipped for irrigation and percentage of cultivated land. Retrieved from http://www.fao.org/nr/water/aquastat/tables/WorldData-Irrigation_eng.pdf

Ferreira, M. I., Silvestre, J., Conceição, N., & Malheiro, A. C. (2012). Crop and stress coefficients in rainfed and deficit irrigation vineyards using sap flow techniques. *Irrigation Science*, *30*(5), 433–447. https://doi.org/10.1007/s00271-012-0352-2

Finnigan, J. J., Clement, R., Malhi, Y., Leuning, R., & Cleugh, H. A. (2003). Techniques Part I: Averaging and coordinate rotation. *Boundary-Layer Meteorology*, *107*, 1–48. https://doi.org/10.1023/a:1021554900225

Flo, V., Martinez-Vilalta, J., Steppe, K., Schuldt, B., & Poyatos, R. (2019). A synthesis of bias and uncertainty in sap flow methods. *Agricultural and Forest Meteorology*, *271*(July 2018), 362–374. https://doi.org/10.1016/j.agrformet.2019.03.012

Foken, T. (2008). The energy balance closure problem: An overview. *Ecological Applications*, *18*(6), 1351–1367. https://doi.org/10.1890/06-0922.1

Foken, T., & Wichura, B. (1996). Tools for quality assessment of surface-based flux measurements. *Agricultural and Forest Meteorology*, *78*(1–2), 83–105. https://doi.org/10.1016/0168-1923(95)02248-1

Gao, L., Zhao, P., Kang, S., Li, S., Tong, L., Ding, R., & Lu, H. (2019). Surface soil water content dominates the difference between ecosystem and canopy water use efficiency in a sparse vineyard. *Agricultural Water Management*, *226*, 105817. https://doi.org/10.1016/j.agwat.2019.105817

Grachev, A. A., Fairall, C. W., Blomquist, B. W., Fernando, H. J. S., Leo, L. S., Otárola-Bustos, S. F., et al. (2020). On the surface energy balance closure at different temporal scales. *Agricultural and Forest Meteorology*, *281*(May 2019), 107823. https://doi.org/10.1016/j.agrformet.2019.107823

Helbig, M., Boike, J., Langer, M., Schreiber, P., Runkle, B. R. K., & Kutzbach, L. (2013). Spatial and seasonal variability of polygonal tundra water balance: Lena River Delta, northern Siberia (Russia). *Hydrogeology Journal*, *21*(1), 133–147. https://doi.org/10.1007/s10040-012-0933-4

19447973, 2025, 3, Downloaded from https://agupubs.onlinelibrary.wiley.com/doi/10.1029/2023WR035360 by CochraneItalia, Wiley Online Library on [28/03/2025]. See the Terms and Conditions (https://onlinelibrary.wiley.com/terms-and-conditions) on Wiley Online Library for rules of use; OA articles are governed by the applicable Creative Commons License

Hossen, M. S., Mano, M., Miyata, A., Baten, M. A., & Hiyama, T. (2012). Surface energy partitioning and evapotranspiration over a double-cropping paddy field in Bangladesh. *Hydrological Processes*, *26*(9), 1311–1320. https://doi.org/10.1002/hyp.8232

Hu, X., & Lei, H. (2021). Evapotranspiration partitioning and its interannual variability over a winter wheat-summer maize rotation system in the North China Plain. *Agricultural and Forest Meteorology*, *310*, 108635. https://doi.org/10.1016/j.agrformet.2021.108635

Hu, Z., Sun, S., Sun, X., Lin, S., Song, C., & Wang, G. (2023). Controlling factors of the spatial-temporal fluctuations in evapotranspiration along an elevation gradient across humid montane ecosystems. *Water Resources Research*, *59*(1). https://doi.org/10.1029/2022WR033228

Ibrom, A., Dellwik, E., Flyvbjerg, H., Jensen, N. O., & Pilegaard, K. (2007). Strong low-pass filtering effects on water vapour flux measurements with closed-path eddy correlation systems. *Agricultural and Forest Meteorology*, *147*(3–4), 140–156. https://doi.org/10.1016/j.agrformet.2007.07.007

IPCC. (2023). Climate change 2023: Synthesis report. In H. Lee & J. Romero (Eds.), *A report of the intergovernmental panel on climate change. Contribution of working groups I, II and III to the sixth assessment report of the intergovernmental panel on climate change [Core writing Team.* IPCC.

Järveoja, J., Nilsson, M. B., Crill, P. M., & Peichl, M. (2020). Bimodal diel pattern in peatland ecosystem respiration rebuts uniform temperature response. *Nature Communications*, *11*(1), 1–10. https://doi.org/10.1038/s41467-020-18027-1

Jiao, L., Lu, N., Fu, B., Wang, J., Li, Z., Fang, W., et al. (2018). Evapotranspiration partitioning and its implications for plant water use strategy: Evidence from a black locust plantation in the semi-arid Loess Plateau, China. *Ecological Management*, *424*, 428–438. https://doi.org/10.1016/j.foreco.2018.05.011

Kidron, G. J., & Starinsky, A. (2019). Measurements and ecological implications of non-rainfall water in desert ecosystems—A review. *Eco-hydrology*, *12*(6). https://doi.org/10.1002/eco.2121

Kljun, N., Calanca, P., Rotach, M. W., & Schmid, H. P. (2015). A simple two-dimensional parameterisation for Flux Footprint Prediction (FFP). *Geoscientific Model Development*, *8*(11), 3695–3713. https://doi.org/10.5194/gmd-8-3695-2015

Klosterhalfen, A., Graf, A., Brüggemann, N., Drüe, C., Esser, O., González-Dugo, M. P., et al. (2019). Source partitioning of H_2O and CO_2 fluxes based on high-frequency eddy covariance data: A comparison between study sites. *Biogeosciences*, *16*(6), 1111–1132. https://doi.org/10.5194/bg-16-1111-2019

Kolle, O., & Rebmann, C. (2007). Technical reports 10: EddySoft documentation of a software package to acquire and process eddy covariance data.

Kool, D., Agam, N., Lazarovitch, N., Heitman, J., Sauer, T., & Ben-Gal, A. (2014). A review of approaches for evapotranspiration partitioning. *Agricultural and Forest Meteorology*, *184*, 56–70. https://doi.org/10.1016/j.agrformet.2013.09.003

Kool, D., Kustas, W. P., Ben-Gal, A., Lazarovitch, N., Heitman, J., Sauer, T., & Agam, N. (2016). Energy and evapotranspiration partitioning in a desert vineyard. *Agricultural and Forest Meteorology*, *218–219*, 277–287. https://doi.org/10.1016/j.agrformet.2016.01.002

Krich, C., Mahecha, M. D., Migliavacca, M., De Kauwe, M. G., Griebel, A., Runge, J., & Miralles, D. G. (2022). Decoupling between ecosystem photosynthesis and transpiration: A last resort against overheating. *Environmental Research Letters*, *17*(4), 044013. https://doi.org/10.1088/1748-9326/ac583e

Kuhn, M. (2008). Building predictive models in R using the caret package. *Journal of Statistical Software*, *28*(5), 1–26. https://doi.org/10.18637/jss.v028.i05

Li, X., Gentine, P., Lin, C., Zhou, S., Sun, Z., Zheng, Y., et al. (2019). A simple and objective method to partition evapotranspiration into transpiration and evaporation at eddy-covariance sites. *Agricultural and Forest Meteorology*, *265*, 171–182. https://doi.org/10.1016/j.agrformet.2018.11.017

LI-COR Team. (2021). SoilFluxProTM software.

Linderson, M.-L., Mikkelsen, T. N., Ibrom, A., Lindroth, A., Ro-Poulsen, H., & Pilegaard, K. (2012). Up-scaling of water use efficiency from leaf to canopy as based on leaf gas exchange relationships and the modeled in-canopy light distribution. *Agricultural and Forest Meteorology*, *152*, 201–211. https://doi.org/10.1016/j.agrformet.2011.09.019

Livingston, G. P., & Hutchinson, G. L. (1995). Enclosure-based measurement of trace gas ex-change: Applications and sources of error. In P. A. Matson & R. Harriss (Eds.), *Biogenic trace gases: Measuring emissions from soil and water* (pp. 14–51). Blackwell Science.

Mancha, L. A., Uriarte, D., Bejarano, M. A., & Prieto, M. H. (2017). Use of sap flow sensors to determine vine transpiration. *Acta Horticulturae*, *1188*, 243–250. https://doi.org/10.17660/ActaHortic.2017.1188.31

Massman, W. J., & Ibrom, A. (2008). Attenuation of concentration fluctuations of water vapor and other trace gases in turbulent tube flow. *8*, 9819–9853. https://doi.org/10.5194/acpd-8-9819-2008

Mauder, M., & Foken, T. (2006). Impact of post-field data processing on eddy covariance flux estimates and energy balance closure. *Meteorologische Zeitschrift*, *15*(6), 597–609. https://doi.org/10.1127/0941-2948/2006/0167

McLeod, M. K., Daniel, H., Faulkner, R., & Murison, R. (2004). Evaluation of an enclosed portable chamber to measure crop and pasture actual evapotranspiration at small scale. *Agricultural Water Management*, *67*(1), 15–34. https://doi.org/10.1016/j.agwat.2003.12.006

Meinshausen, N. (2006). Quantile regression for left-truncated semicompeting risks data. *Journal of Machine Learning Research*, *7*, 983–999. https://doi.org/10.1111/j.1541-0420.2010.01521.x

Miralles, D. G., Gentine, P., Seneviratne, S. I., & Teuling, A. J. (2018). Land–atmospheric feedbacks during droughts and heatwaves: State of the science and current challenges. *Annals of the New York Academy of Sciences*, *1436*(1), 19–35. https://doi.org/10.1111/nyas.13912

Montagnani, L., Zanotelli, D., Tagliavini, M., & Tomelleri, E. (2018). Timescale effects on the environmental control of carbon and water fluxes of an apple orchard. *Ecology and Evolution*, *8*(1), 416–434. https://doi.org/10.1002/ece3.3633

Nelson, J. A., Carvalhais, N., Cuntz, M., Delpierre, N., Knauer, J., Ogée, J., et al. (2018). Coupling water and carbon fluxes to constrain estimates of transpiration: The TEA algorithm. *Journal of Geophysical Research: Biogeosciences*, *123*(12), 3617–3632. https://doi.org/10.1029/2018JG004727

Nelson, J. A., Pérez-Priego, O., Zhou, S., Poyatos, R., Zhang, Y., Blanken, P. D., et al. (2020). Ecosystem transpiration and evaporation: Insights from three water flux partitioning methods across FLUXNET sites. *Global Change Biology*, *26*(12), 6916–6930. https://doi.org/10.1111/gcb.15314

Nordbo, A., Kekäläinen, P., Siivola, E., Lehto, R., Vesala, T., & Timonen, J. (2013). Tube transport of water vapor with condensation and desorption. *Applied Physics Letters*, *102*(19). https://doi.org/10.1063/1.4804639

Papale, D., Reichstein, M., Aubinet, M., Canfora, E., Bernhofer, C., Kutsch, W., et al. (2006). Towards a standardized processing of Net Ecosystem Exchange measured with eddy covariance technique: Algorithms and uncertainty estimation. *Biogeosciences*, *3*(4), 571–583. https://doi.org/10.5194/bg-3-571-2006

Paul-Limoges, E., Revill, A., Maier, R., Buchmann, N., & Damm, A. (2022). Insights for the partitioning of ecosystem evaporation and transpiration in short-statured croplands. *Journal of Geophysical Research: Biogeosciences*, *127*(7), 1–19. https://doi.org/10.1029/2021JG006760

19447973, 2025, 3, Downloaded from https://agupubs.onlinelibrary.wiley.com/doi/10.1029/2023WR035360 by CochraneItalia, Wiley Online Library on [28/03/2025]. See the Terms and Conditions (https://onlinelibrary.wiley.com/terms-and-conditions) on Wiley Online Library for rules of use; OA articles are governed by the applicable Creative Commons License

Paul-Limoges, E., Wolf, S., Schneider, F. D., Longo, M., Moorcroft, P., Gharun, M., & Damm, A. (2020). Partitioning evapotranspiration with concurrent eddy covariance measurements in a mixed forest. *Agricultural and Forest Meteorology*, *280*, 107786. https://doi.org/10.1016/j.agrformet.2019.107786

Paulus, S. J., El-Madany, T. S., Orth, R., Hildebrandt, A., Wutzler, T., Carrara, A., et al. (2022). Resolving seasonal and diel dynamics of non-rainfall water inputs in a Mediterranean ecosystem using lysimeters. *Hydrology and Earth System Sciences*, *26*(23), 6263–6287. https://doi.org/10.5194/hess-26-6263-2022

Peressotti, A., & Ham, J. M. (1996). A dual-heater gauge for measuring sap flow with an improved heat-balance method. *Agronomy Journal*, *155*(2), 149–155. https://doi.org/10.2134/agronj1996.00021962008800020006x

Poblete-Echeverría, C. A., & Ortega-Farias, S. O. (2013). Evaluation of single and dual crop coefficients over a drip-irrigated Merlot vineyard (Vitis viniferaL.) using combined measurements of sap flow sensors and an eddy covariance system. *Australian Journal of Grape and Wine Research*, *19*(2), 249–260. https://doi.org/10.1111/ajgw.12019

Qubaja, R., Amer, M., Tatarinov, F., Rotenberg, E., Preisler, Y., Sprintsin, M., & Yakir, D. (2020). Partitioning evapotranspiration and its long-term evolution in a dry pine forest using measurement-based estimates of soil evaporation. *Agricultural and Forest Meteorology*, *281*, 107831. https://doi.org/10.1016/j.agrformet.2019.107831

Rafi, Z., Merlin, O., Le Dantec, V., Khabba, S., Mordelet, P., Er-Raki, S., et al. (2019). Partitioning evapotranspiration of a drip-irrigated wheat crop: Inter-comparing eddy covariance-sap flow-lysimeter- and FAO-based methods. *Agricultural and Forest Meteorology*, *265*, 310–326. https://doi.org/10.1016/j.agrformet.2018.11.031

Raghav, P., Wagle, P., Kumar, M., Banerjee, T., & Neel, J. P. S. (2022). Vegetation index-based partitioning of evapotranspiration is deficient in grazed systems. *Water Resources Research*, *58*(8). https://doi.org/10.1029/2022wr032067

Raz-Yaseef, N., Rotenberg, E., & Yakir, D. (2010). Effects of spatial variations in soil evaporation caused by tree shading on water flux partitioning in a semi-arid pine forest. *Agricultural and Forest Meteorology*, *150*(3), 454–462. https://doi.org/10.1016/j.agrformet.2010.01.010

R Core Team. (2021). R: A language and environment for statistical computing.

Reichstein, M., Camps-Valls, G., Stevens, B., Jung, M., Denzler, J., Carvalhais, N., & Prabhat, F. (2019). Deep learning and process understanding for data-driven Earth system science. *Nature*, *566*(7743), 195–204. https://doi.org/10.1038/s41586-019-0912-1

Reichstein, M., Falge, E., Baldocchi, D., Papale, D., Aubinet, M., Berbigier, P., et al. (2005). On the separation of net ecosystem exchange into assimilation and ecosystem respiration: Review and improved algorithm. *Global Change Biology*, *11*(9), 1424–1439. https://doi.org/10.1111/j.1365-2486.2005.001002.x

Runkle, B. R. K., Wille, C., Gažovič, M., & Kutzbach, L. (2012). Attenuation correction procedures for water vapour fluxes from closed-path eddy-covariance systems. *Boundary-Layer Meteorology*, *142*(3), 401–423. https://doi.org/10.1007/s10546-011-9689-y

Sakuratani, T. (1981). A heat balance method for measuring water flux in the stem of intact plants. *Journal of Agricultural Meteorology*, *37*(1), 9–17. https://doi.org/10.2480/agrmet.37.9

Sánchez, J. M., López-Urrea, R., Valentín, F., Caselles, V., & Galve, J. M. (2019). Lysimeter assessment of the Simplified Two-Source Energy Balance model and eddy covariance system to estimate vineyard evapotranspiration. *Agricultural and Forest Meteorology*, *274*, 172–183. https://doi.org/10.1016/j.agrformet.2019.05.006

Scanlon, T. M., & Kustas, W. P. (2010). Partitioning carbon dioxide and water vapor fluxes using correlation analysis. *Agricultural and Forest Meteorology*, *150*(1), 89–99. https://doi.org/10.1016/j.agrformet.2009.09.005

Scott, R. L., Knowles, J. F., Nelson, J. A., Gentine, P., Li, X., Barron-Gafford, G., et al. (2021). Water availability impacts on evapotranspiration partitioning. *Agricultural and Forest Meteorology*, *297*, 108251. https://doi.org/10.1016/j.agrformet.2020.108251

Shtai, W., Asensio, D., Kadison, A. E., Schwarz, M., Raifer, B., Andreotti, C., et al. (2024). Soil water availability modulates the response of grapevine leaf gas exchange and PSII traits to a simulated heat wave. *Plant and Soil*, *501*(1–2), 537–554. https://doi.org/10.1007/s11104-024-06536-7

Shuttleworth, W. J., & Wallace, J. S. (1985). Evaporation from sparse crops-an energy combination theory. *Quarterly Journal of the Royal Meteorological Society*, *111*(469), 839–855. https://doi.org/10.1002/qj.49711146510

Simpson, G., Runkle, B. R. K., Eckhardt, T., & Kutzbach, L. (2019). Evaluating closed chamber evapotranspiration estimates against eddy covariance measurements in an arctic wetland. *Journal of Hydrology*, *578*, 124030. https://doi.org/10.1016/j.jhydrol.2019.124030

Soubie, R., Heinesch, B., Granier, A., Aubinet, M., & Vincke, C. (2016). Evapotranspiration assessment of a mixed temperate forest by four methods: Eddy covariance, soil water budget, analytical and model. *Agricultural and Forest Meteorology*, *228*(229), 191–204. https://doi.org/10.1016/j.agrformet.2016.07.001

Stekhoven, D. J., & Buehlmann, P. (2012). MissForest - Nonparametric missing value imputation for mixed-type data (pp. 112–118).

Stoy, P. C., El-Madany, T. S., Fisher, J. B., Gentine, P., Gerken, T., Good, S. P., et al. (2019). Reviews and syntheses: Turning the challenges of partitioning ecosystem evaporation and transpiration into opportunities. *Biogeosciences*, *16*(19), 3747–3775. https://doi.org/10.5194/bg-16-3747-2019

Stoy, P. C., Mauder, M., Foken, T., Marcolla, B., Boegh, E., Ibrom, A., et al. (2013). A data-driven analysis of energy balance closure across FLUXNET research sites: The role of landscape scale heterogeneity. *Agricultural and Forest Meteorology*, *171–172*, 137–152. https://doi.org/10.1016/j.agrformet.2012.11.004

Tamburini, G., Bommarco, R., Wanger, T. C., Kremen, C., van der Heijden, M. G. A., Liebman, M., & Hallin, S. (2020). Agricultural diversification promotes multiple ecosystem services without compromising yield. *Science Advances*, *6*(45), eaba1715. https://doi.org/10.1126/sciadv.aba1715

Taylor, J. (1997). *Introduction to error analysis, the study of uncertainties in physical measurements*. University Science Books.

Teuling, A. J., Hirschi, M., Ohmura, A., Wild, M., Reichstein, M., Ciais, P., et al. (2009). Regional radiation impacts on evapotranspiration trends. *Geophysical Research Letters*, *36*(2), L02404. https://doi.org/10.1029/2008GL036584

Teuling, A. J., Seneviratne, S. I., Stöckli, R., Reichstein, M., Moors, E., Ciais, P., et al. (2010). Contrasting response of European forest and grassland energy exchange to heatwaves. *Nature Geoscience*, *3*(10), 722–727. https://doi.org/10.1038/ngeo950

Tezza, L., Vendrame, N., & Pitacco, A. (2019). Disentangling the carbon budget of a vineyard: The role of soil management. *Agriculture, Ecosystems & Environment*, *272*, 52–62. https://doi.org/10.1016/j.agee.2018.11.002

Thiery, W., Visser, A. J., Fischer, E. M., Hauser, M., Hirsch, A. L., Lawrence, D. M., et al. (2020). Warming of hot extremes alleviated by expanding irrigation. *Nature Communications*, *11*(1), 290. https://doi.org/10.1038/s41467-019-14075-4

Tong, Y., Wang, P., Li, X.-Y., Wang, L., Wu, X., Shi, F., et al. (2019). Seasonality of the transpiration fraction and its controls across typical ecosystems within the Heihe river basin. *Journal of Geophysical Research: Atmospheres*, *124*(3), 1277–1291. https://doi.org/10.1029/2018JD029680

19447973, 2025, 3, Downloaded from https://agupubs.onlinelibrary.wiley.com/doi/10.1029/2023WR035360 by CochraneItalia, Wiley Online Library on [28/03/2025]. See the Terms and Conditions (https://onlinelibrary.wiley.com/terms-and-conditions) on Wiley Online Library for rules of use; OA articles are governed by the applicable Creative Commons License

Trambouze, W., Bertuzzi, P., & Voltz, M. (1998). Comparison of methods for estimating actual evapotranspiration in a row-cropped vineyard. *Agricultural and Forest Meteorology*, *91*(3–4), 193–208. https://doi.org/10.1016/S0168-1923(98)00072-0

Tricker, P. J., Pecchiari, M., Bunn, S. M., Vaccari, F. P., Peressotti, A., Miglietta, F., & Taylor, G. (2009). Water use of a bioenergy plantation increases in a future high CO2 world. *Biomass and Bioenergy*, *33*(2), 200–208. https://doi.org/10.1016/j.biombioe.2008.05.009

Vandegehuchte, M. W., & Steppe, K. (2013). Sap-flux density measurement methods: Working principles and applicability. *Functional Plant Biology*, *40*(3), 213–223. https://doi.org/10.1071/FP12233

Van Eerd, L. L., Chahal, I., Peng, Y., & Awrey, J. C. (2023). Influence of cover crops at the four spheres: A review of ecosystem services, potential barriers, and future directions for north America. *Science of the Total Environment*, *858*(Part 3), 159990. https://doi.org/10.1016/j.scitotenv.2022.159990

Varolo, E., Zanotelli, D., Montagnani, L., Tagliavini, M., & Zerbe, S. (2016). Colonization of a deglaciated moraine: Contrasting patterns of carbon uptake and release from C3 and CAM plants. *PLoS One*, *11*(12), 1–24. https://doi.org/10.1371/journal.pone.0168741

Villalobos, F. J., & Fereres, E. (2016). Principles of agronomy for sustainable agriculture.

Virkkala, A. M., Aalto, J., Rogers, B. M., Tagesson, T., Treat, C. C., Natali, S. M., et al. (2021). Statistical upscaling of ecosystem CO_2 fluxes across the terrestrial tundra and boreal domain: Regional patterns and uncertainties. *Global Change Biology*, *27*(17), 4040–4059. https://doi.org/10.1111/gcb.15659

Vukicevich, E., Lowery, T., Bowen, P., Úrbez-Torres, J. R., & Hart, M. (2016). Cover crops to increase soil microbial diversity and mitigate decline in perennial agriculture. A review. *Agronomy for Sustainable Development*, *36*(3), 48. https://doi.org/10.1007/s13593-016-0385-7

Wei, Z., Lee, X., Wen, X., & Xiao, W. (2018). Evapotranspiration partitioning for three agro-ecosystems with contrasting moisture conditions: A comparison of an isotope method and a two-source model calculation. *Agricultural and Forest Meteorology*, *252*, 296–310. https://doi.org/10.1016/j.agrformet.2018.01.019

Wei, Z., Yoshimura, K., Wang, L., Miralles, D. G., Jasechko, S., & Lee, X. (2017). Revisiting the contribution of transpiration to global terrestrial evapotranspiration: Revisiting global ET partitioning. *Geophysical Research Letters*, *44*(6), 2792–2801. https://doi.org/10.1002/2016GL072235

Wenter, A., Zanotelli, D., Montagnani, L., Tagliavini, M., & Andreotti, C. (2018). Effect of different timings and intensities of water stress on yield and berry composition of grapevine (cv. Sauvignon blanc) in a mountain environment. *Scientia Horticulturae*, *236*, 137–145. https://doi.org/10.1016/j.scienta.2018.03.037

Wilson, K., Falge, E., Aubinet, M., & Baldocchi, D. (2002). DigitalCommons @ University of Nebraska - Lincoln energy balance closure at FLUXNET sites. *Agricultural and Forest Meteorology*, 223–243.

Wohlfahrt, G., Haslwanter, A., Hörtnagl, L., Jasoni, R. L., Fenstermaker, L. F., Arnone, J. A., III, & Hammerle, A. (2009). On the consequences of the energy imbalance for calculating surface conductance to water vapour. *Agricultural and Forest Meteorology*, *149*(9), 1556–1559. https://doi.org/10.1016/j.agrformet.2009.03.015

Wutzler, T., Lucas-Moffat, A., Migliavacca, M., Knauer, J., Sickel, K., Šigut, L., et al. (2018). Basic and extensible post-processing of eddy covariance flux data with REddyProc. *Biogeosciences Discussions*, 1–39. https://doi.org/10.5194/bg-2018-56

Yu, L., Zhou, S., Zhao, X., Gao, X., Jiang, K., Zhang, B., et al. (2022). Evapotranspiration partitioning based on leaf and ecosystem water use efficiency. *Water Resources Research*, *58*(9). https://doi.org/10.1029/2021WR030629

Yu, X., Orth, R., Reichstein, M., Bahn, M., Klosterhalfen, A., Knohl, A., et al. (2022). Contrasting drought legacy effects on gross primary productivity in a mixed versus pure beech forest. *Biogeosciences*, *19*(17), 4315–4329. https://doi.org/10.5194/bg-19-4315-2022

Yue, P., Zhang, Q., Ren, X., Yang, Z., Li, H., & Yang, Y. (2022). Environmental and biophysical effects of evapotranspiration in semiarid grassland and maize cropland ecosystems over the summer monsoon transition zone of China. *Agricultural Water Management*, *264*, 107462. https://doi.org/10.1016/j.agwat.2022.107462

Zanotelli, D., Montagnani, L., Andreotti, C., & Tagliavini, M. (2019). Evapotranspiration and crop coefficient patterns of an apple orchard in a sub-humid environment. *Agricultural Water Management*, *226*, 105756. https://doi.org/10.1016/j.agwat.2019.105756

Zhang, J., Liu, J., Yang, C., Du, S., & Yang, W. (2016). Photosynthetic performance of soybean plants to water deficit under high and low light intensity. *South African Journal of Botany*, *105*, 279–287. https://doi.org/10.1016/j.sajb.2016.04.011

Zhang, W., Jung, M., Migliavacca, M., Poyatos, R., Miralles, D. G., El-Madany, T. S., et al. (2023). The effect of relative humidity on eddy covariance latent heat flux measurements and its implication for partitioning into transpiration and evaporation Agricultural and Forest Meteorology the effect of relative humidity on eddy covariance latent heat flu. *Agricultural and Forest Meteorology*, *330*, 109305. https://doi.org/10.1016/j.agrformet.2022.109305

Zhang, Y., Kang, S., Ward, E. J., Ding, R., Zhang, X., & Zheng, R. (2011). Evapotranspiration components determined by sap flow and microlysimetry techniques of a vineyard in northwest China: Dynamics and influential factors. *Agricultural Water Management*, *98*(8), 1207–1214. https://doi.org/10.1016/j.agwat.2011.03.006

Zhao, P., Hammerle, A., Zeeman, M., & Wohlfahrt, G. (2018). On the calculation of daytime CO2 fluxes measured by automated closed transparent chambers. *Agricultural and Forest Meteorology*, *263*, 267–275. https://doi.org/10.1016/j.agrformet.2018.08.022

Zhao, P., Kang, S., Li, S., Ding, R., Tong, L., & Du, T. (2018). Seasonal variations in vineyard ET partitioning and dual crop coefficients correlate with canopy development and surface soil moisture. *Agricultural Water Management*, *197*, 19–33. https://doi.org/10.1016/j.agwat.2017.11.004

Zhao, P., Li, S., Li, F., Du, T., Tong, L., & Kang, S. (2015). Comparison of dual crop coefficient method and Shuttleworth – Wallace model in evapotranspiration partitioning in a vineyard of northwest China. *Agricultural Water Management*, *160*, 41–56. https://doi.org/10.1016/j.agwat.2015.06.026

Zhou, S., Yu, B., Zhang, Y., Huang, Y., & Wang, G. (2016). Partitioning evapotranspiration based on the concept of underlying water use efficiency. *Journal of the American Water Resources Association*, *52*(2), 1160–1175. https://doi.org/10.1111/j.1752-1688.1969.tb04897.x

References From the Supporting Information

Forbrich, I., Kutzbach, L., Hormann, A., & Wilmking, M. (2010). A comparison of linear and exponential regression for estimating diffusive CH4 fluxes by closed-chambers in peatlands. *Soil Biology and Biochemistry*, *42*(3), 507–515. https://doi.org/10.1016/j.soilbio.2009.12.004

Kutzbach, L., Schneider, J., Sachs, T., Giebels, M., Nykänen, H., Shurpali, N. J., et al. (2007). CO_2 flux determination by closed-chamber methods can be seriously biased by inappropriate application of linear regression. *Biogeosciences*, *4*(6), 1005–1025. https://doi.org/10.5194/bg-4-1005-2007

LI-COR, I. (2015). Using the LI-8100A soil gas flux system (pp. 1–220).

19447973, 2025, 3, Downloaded from https://agupubs.onlinelibrary.wiley.com/doi/10.1029/2023WR035360 by CochraneItalia, Wiley Online Library on [28/03/2025]. See the Terms and Conditions (https://onlinelibrary.wiley.com/terms-and-conditions) on Wiley Online Library for rules of use; OA articles are governed by the applicable Creative Commons License

Verhoef, A., Diaz-Espejo, A., Knight, J. R., Villagarcía, L., & Fernández, J. E. (2006). Adsorption of water vapor by bare soil in an olive grove in southern Spain. *Journal of Hydrometeorology*, *7*(5), 1011–1027. https://doi.org/10.1175/JHM556.1

Zanotelli, D., Montagnani, L., Manca, G., & Tagliavini, M. (2013). Net primary productivity, allocation pattern and carbon use efficiency in an apple orchard assessed by integrating eddy covariance, biometric and continuous soil chamber measurements. *Biogeosciences*, *10*(5), 3089–3108. https://doi.org/10.5194/bg-10-3089-2013

19447973, 2025, 3, Downloaded from https://agupubs.onlinelibrary.wiley.com/doi/10.1029/2023WR035360 by CochraneItalia, Wiley Online Library on [28/03/2025]. See the Terms and Conditions (https://onlinelibrary.wiley.com/terms-and-conditions) on Wiley Online Library for rules of use; OA articles are governed by the applicable Creative Commons License